

# Review of Light-Activated Antimicrobial Nanoparticle–Polymer Composites for Biomedical Devices

Mina Omidian, Pannaree Srinoi, Pooria Tajalli, and T. Randall Lee\*

Cite This: *ACS Appl. Nano Mater.* 2024, 7, 8377–8391

Read Online

ACCESS |

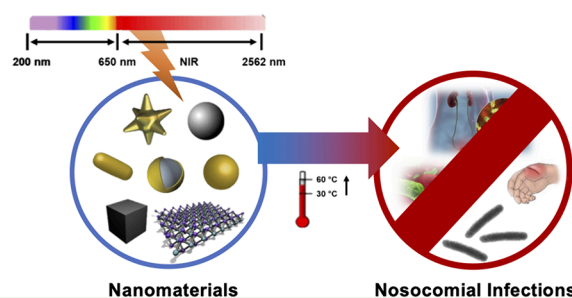
Metrics &amp; More

Article Recommendations

**ABSTRACT:** Nosocomial infections are a significant threat to public health that leads to substantial morbidity and mortality. The emergence and spread of antibiotic-resistant organisms have compounded the complexity of managing these infections, highlighting the urgent need for innovative and effective strategies to combat them. Photostimuli-responsive nanomaterials have emerged as promising tools for coating biomedical devices and tools against nosocomial infections due to their ability to selectively target and kill pathogenic bacteria and fungi. It is feasible to develop antibacterial surfaces by integrating photothermal agents (PTAs), photodynamic agents (PDAs), and both PTAs and PDAs into coatings. When exposed to light, PTAs generate heat that can be used to kill bacteria, while PDAs emit reactive oxygen species (ROS) that can also be used to kill bacteria. The combination of photothermal and photodynamic therapies produces a synergistic effect in which the death of bacteria is boosted in comparison with the use of each individual therapy. These coatings have the potential to provide enhanced bacterial control for a number of biomedical devices, including implants, catheters, meshes, and wound dressings. The utilization of antimicrobial nanomaterials offers a promising approach for reducing the risk of infections associated with the use of these devices.

**KEYWORDS:** photodynamic therapy (PDT), photothermal therapy (PTT), polymer, nanomaterial, nosocomial infections, light, antimicrobial, biomedical devices

## Light-Activated Antimicrobial Nanoparticle–Polymer Composites



## 1. INTRODUCTION

Nosocomial infections, often known as hospital-acquired infections (HAIs), represent a worldwide problem, giving rise to significant financial concerns for hospitals as well as health risks for patients.<sup>1</sup> These infections occur in patients who are hospitalized, as well as in outpatients receiving care in clinics, surgery centers, and other settings.<sup>2</sup> The National Health Safety Network and Centers for Disease Control and Prevention classify nosocomial infections into 14 distinct categories.<sup>1</sup> HAIs caused by devices are the most prevalent in healthcare settings with adhesion of microorganisms and formation of biofilms on the surface of medical devices.<sup>1,3,4</sup> Nosocomial infections including urinary tract infections, pneumonia, and surgical-site infections<sup>5</sup> can be caused by a number of microorganisms, including bacteria, viruses, and fungi. Additionally, the microorganisms can be transmitted by contact with contaminated surfaces or equipment, as well as through direct contact with infected patients or healthcare personnel.<sup>2</sup>

To prevent the transmission of nosocomial infections, it is essential to practice proper hand hygiene, clean and disinfect equipment and surfaces, and isolate patients who are infected.<sup>1</sup> The development of antibiotics has had a significant impact on

the treatment of infectious diseases throughout the past few decades. However, the misuse and overuse of antibiotics have also contributed to the creation of antibiotic-resistant bacterial strains.<sup>6,7</sup> Antimicrobial resistance (AMR), particularly due to biofilm development, is one of the most significant obstacles in the treatment of bacterial-infected disorders.<sup>6</sup> According to the World Health Organization, multidrug-resistant (MDR) bacteria kill approximately 700000 people per year on a global level, with the figure is expected to reach 10 million by 2050.<sup>8–10</sup> Due to the cost and complexity of generating new antibiotics, scientists are refocusing their efforts on antibacterial techniques with a lower risk of AMR development.

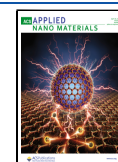
Antibacterial methods based on nanoparticles have been reported as highly efficient against infections caused by biofilms.<sup>11</sup> Among nanomaterial-based treatments, phototherapy has attracted a great deal of interest due to its obvious

Received: October 30, 2023

Revised: March 9, 2024

Accepted: March 12, 2024

Published: April 8, 2024



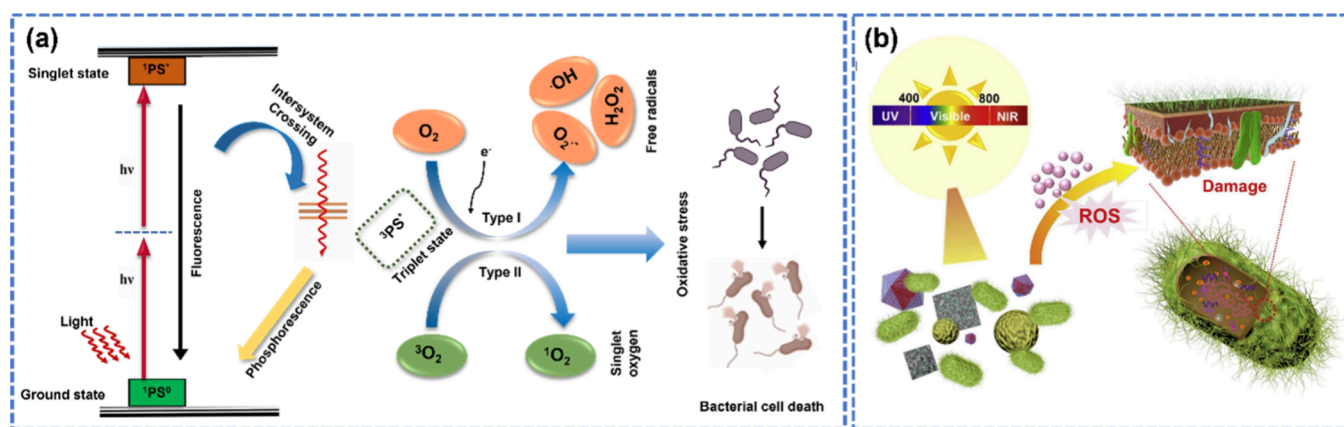


**Figure 1.** (a) Illustration of the Type I and Type II photochemical mechanisms of APDT (Jablonski diagram). (b) Schematic illustration of the mechanism of bacterial damage. Reprinted with permission from ref 65. Copyright 2020 Elsevier.

advantages of minimum invasiveness and clinical safety. In general, photoactivated sterilization can be simplified by activating photostimuli-responsive nanomaterials with light wavelengths ranging from ultraviolet (UV) to near-infrared (NIR). These photostimuli-responsive nanomaterials absorb light energy, thereby inhibiting the growth of pathogens via photodynamic therapy (PDT) by producing reactive oxygen species (ROS) and/or photothermal therapy (PTT) by establishing hyperthermic conditions.<sup>12,13</sup>

Developing antibacterial biomedical devices by coating them with photothermal agents (PTAs), photodynamic agents (PDAs) or a mixture of PTA and PDA agents is a novel strategy for combating nosocomial infections and enhancing biomedical device resistance to bacterial growth.<sup>14</sup> These devices may include implantable devices such as prosthetic implants,<sup>15,16</sup> prosthetic joints,<sup>17</sup> and orthopedic implants,<sup>18,19</sup> as well as external devices such as catheters<sup>20–27</sup> and wound dressings.<sup>28–32</sup> Antibacterial nanomaterial-based coatings applied to these devices can reduce the risk of infection and improve patient outcomes. The unique properties of light-activated antimicrobial nanoparticle–polymer composites offer multifaceted advantages from a biomedical perspective. By the incorporation of these coatings, the devices gain a robust defense mechanism against microbial colonization, thereby minimizing the potential for device-related infections. The controlled release of antimicrobial agents upon exposure to light not only provides targeted pathogen eradication but also contributes to the overall reduction in the microbial load on the device surface.<sup>11</sup> This reduction in the microbial burden is instrumental in inhibiting biofilm formation, a common precursor to persistent infections associated with implanted biomedical devices. The biocompatibility of these coatings is carefully optimized to ensure minimal cytotoxicity, facilitating seamless integration with biological tissues and reducing the likelihood of adverse reactions. As a result, the application of light-activated antimicrobial nanoparticle–polymer composites as coatings on biomedical devices represents a strategic and innovative approach to elevate patient safety, reduce the incidence of infections, and ultimately enhance the overall efficacy of medical interventions. Although previous literature studies on light-assisted antibacterial activities have been reported, no comprehensive review of light-assisted antimicrobial strategies for biomedical devices has been conducted. This review aims to provide a comprehensive overview of recent advancements in photostimuli-responsive nanomaterial sys-

tems for the development of smart nanomaterial–polymer composites with antibacterial activity for use in biomedical devices. By systematically analyzing the latest research findings from diverse sources, we aim to provide a consolidated and up-to-date understanding of the state-of-the-art in this field. The novelty of our work lies in the meticulous curation of recent literature, which not only summarizes the current landscape but also highlights emerging trends and challenges. This review serves as a valuable resource for researchers, practitioners, and scholars seeking an in-depth and holistic perspective on antimicrobial nanoparticle–polymer composites. Antibacterial modes in these studies are categorized into three types: (1) ROS-based PDT, (2) hyperthermia-based PTT, and (3) a dual photoresponsive therapy system (PDT/PTT). The fabrication and antibacterial activities of some typical PDAs, photosensitizers (PSs), and PTAs are discussed. In addition, several nanomaterial–polymer composites with targeting properties and sensitivity to light and bacterial infections are covered. Finally, the prospects and challenges associated with antibacterial PTT and PDT approaches are addressed.

## 2. LIGHT-ACTIVATED ANTIMICROBIAL NANOPARTICLE–POLYMER COMPOSITES

### 2.1. Photodynamic Antimicrobial Nanoparticle–Polymer Composites.

#### 2.1.1. Mechanism of Antimicrobial Photodynamic Therapy (APDT).

Photodynamic treatment (PDT) has emerged as a promising method for eliminating microorganisms such as bacteria, fungus, viruses, and spores.<sup>33–36</sup> It requires the administration of a PS with a small energy band gap (difference between the valence band and conduction band).<sup>35,37</sup> In a typical APDT, the PS absorbs visible/NIR photons and excites to its high-energy single state ( $^1PS^0$ ). However, excited electrons are unstable and have a short lifetime. The excited molecule ( $^1PS^*$ ) may undergo redox reactions or intersystem crossing in order to produce a triplet state with a longer lifespan ( $^3PS^*$ ).<sup>35,38</sup> When the  $^3PS^*$  and substrate are in close proximity, photochemical reactions proceed via Type I or Type II pathways, as depicted in Figure 1a. In the Type I reaction,  $^3PS^*$  transfers an electron to a substrate, typically molecular oxygen, and initiates the formation of highly reactive superoxide anion ( $O_2^{\bullet-}$ ) and hydroxyl ( $\bullet OH$ ) radicals.<sup>39</sup> All of these ROS are capable of causing irreversible oxidative damage to bacterial cell membranes and other functional biomolecules, including DNA, endoenzymes, proteins, and fatty acids.<sup>39,40</sup> In the

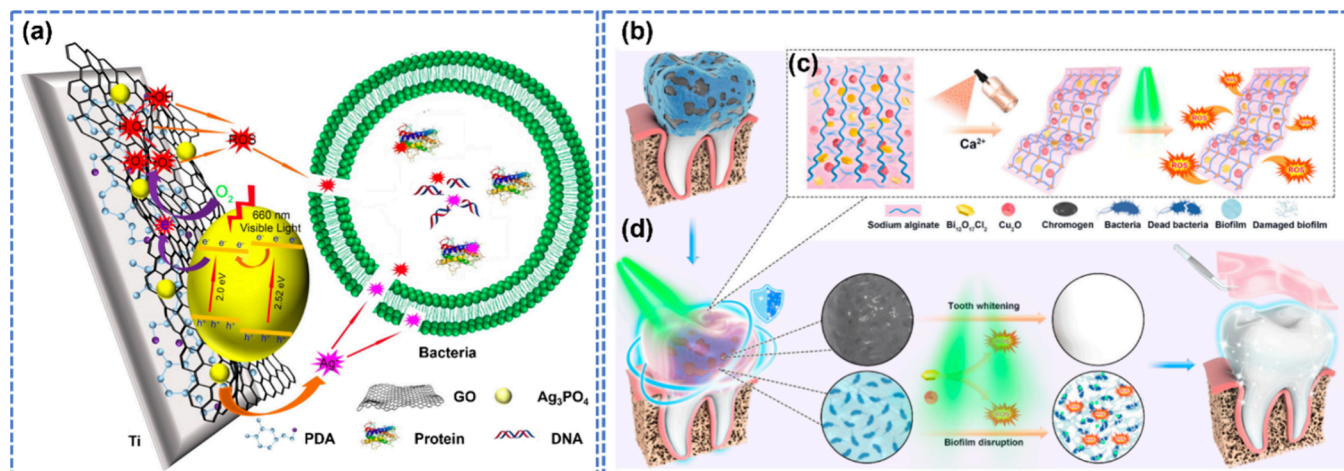


**Figure 2.** (a) Illustration of the synergistic bacteria-killing behavior of  $\text{Ag}^+$  and ROS produced by the hybrid  $\text{Ag}_3\text{PO}_4/\text{GO}$  coating, which combines with titanium by PDA under irradiation with 660 nm visible light, leading to damage of the bacterial cell membranes, proteins, and DNA. Adapted with permission from ref 18. Copyright 2018 American Chemical Society. (b) Schematic illustration of the construction of BC-SA and the working principle. (c) Solution of SA containing  $\text{Bi}_{12}\text{O}_{17}\text{Cl}_{12}$  and  $\text{Cu}_2\text{O}$  cross-linked with  $\text{Ca}^{2+}$ . (d) BC-SA produces ROS under GL for localized biofilm disruption and tooth whitening. Reproduced with permission from ref 51. Copyright 2022 American Chemical Society.

Type II reaction, the excited  $^3\text{PS}^*$  combines with molecular oxygen and forms electronically highly reactive singlet oxygen ( $^1\text{O}_2$ ). The generated  $^1\text{O}_2$  can destroy bacterial pathogens by initiating photodynamic action, which deactivates cellular antioxidants and enhances cell-killing effects mediated by oxidative stress.<sup>35,38</sup> It has been determined that Type I and Type II reactions occur simultaneously in APDT and that their ratio is primarily dependent on the type of PSs and the microenvironment of infected sites.<sup>14</sup> Compared to other therapeutic strategies described in the scientific literature, APDT kills MDR bacterial infections more rapidly. Importantly, the ROS generated by PSs have a multitarget effect on the cellular architecture and metabolic processes of bacteria.<sup>41</sup> Therefore, the APDT platform can be used to manufacture polymeric functional materials for eradicating MDR bacterial infections in chronic wounds, implants, and medical devices.

**2.1.2. Photodynamic Antimicrobial Nanomaterial–Polymer Composites.** In addition to light and oxygen, PSs are a necessary factor for PDT.<sup>42</sup> However, most traditional PSs (dyes) are extremely insoluble, are hydrophobic, and have low stability, which leads to the limited efficiency of PDT.<sup>43</sup> To overcome these difficulties, researchers have investigated the use of photosensitizing nanoparticles alone and in conjunction with other PSs.<sup>44–46</sup> Moreover, nanoparticles are known to have unique optical properties that make them highly efficient at absorbing light, and as a result, they can generate more ROS than traditional dyes. This is due to their small size and large surface area, which allow for more interactions with light and a higher degree of energy transfer.<sup>47</sup> On the basis of this finding, Macdonald and co-workers designed antibacterial surfaces using thiol-capped gold nanoparticles (AuNPs) encapsulated in crystal violet (CV)-coated polyurethane (PU) to evaluate the antibacterial activity against both *Staphylococcus aureus* and *Escherichia coli* as representatives of Gram-positive and Gram-negative bacteria, respectively.<sup>23</sup> The results indicated that the effectiveness of this antibacterial surface was strongly reliant on the size and concentration of the nanoparticles. The most effective PU–AuNPs–CV antibacterial surfaces were achieved with a swell encapsulation concentration of  $1.0 \text{ mg mL}^{-1}$  of 2 nm AuNPs. Essentially, *S. aureus* and *E. coli* were reduced

below the detection limit ( $>4 \log$ ) after 2 h in the dark and light irradiation.<sup>23</sup>

In a separate study, the antibacterial activity of PU polymers (as a model for catheters) against *S. aureus* bacteria was investigated.<sup>20</sup> In this study, PU polymers were exposed to white light for 24 h. The antibacterial test confirmed that the antibacterial capabilities of polymers impregnated with PSs alone were lower than those of polymers embedded with nanogold particles and PSs.<sup>20</sup> Interestingly, a bimetallic@photosensitizer nanoconjugate system was utilized by Chandna and co-workers. They recently reported a bioinspired nanantimicrobial hydrogel for wound treatment against *Candida tropicalis*.<sup>28</sup> In this study, stable poly(acrylic acid)-based hydrogels were embedded with rose bengal (RB), as a PS, loaded with lignin-based gold and silver bimetallic nanoconjugates (AuAgLNCs); additionally, the photodynamic antifungal activity of this hydrogel (RB@AuAgLNCs) was determined to have the highest percentage of fungal growth inhibition with a very low  $\text{IC}_{50}$  value ( $0.1 \mu\text{g mL}^{-1}$ ).<sup>28</sup> The addition of silver nanoparticles and graphene into a polymer has been proven to have significant antibacterial activity in biomedical devices.<sup>48,49</sup> Regarding the coating of biomedical implants, Xie, Mao, and co-workers developed a controllable, rapid, and effective in situ disinfection approach.<sup>18</sup> In this study, a hybrid polydopamine (PDA)/ $\text{Ag}_3\text{NO}_4$ /graphene oxide (GO) coating was designed to achieve rapid bacteria killing and biofilm elimination in situ via the synergistic actions of  $\text{Ag}^+$  and ROS produced by the  $\text{Ag}_3\text{PO}_4$  nanoparticles under 660 nm visible light by tuning the band gap of the  $\text{Ag}_3\text{PO}_4$  nanoparticles with GO, as shown in Figure 2a.<sup>18</sup> Therefore,  $\text{Ag}^+$  and ROS can damage DNA and proteins synergistically. In addition, PDA is compatible with a range of materials, so the method is relevant not only to metallic implants but also to biopolymers such as poly(ether ether ketone) (PEEK). The PDA/ $\text{Ag}_3\text{PO}_4$ /GO hybrid coating exhibited high antibacterial efficiencies of 99.53% and 99.66% against *E. coli* and *S. aureus*, respectively.<sup>18</sup>

In addition, attention has been drawn to inorganic metal oxide nanoparticles such as titanium oxide ( $\text{TiO}_2$ ), zinc oxide ( $\text{ZnO}$ ), and cubic cuprous oxide ( $\text{Cu}_2\text{O}$ ), which exhibit

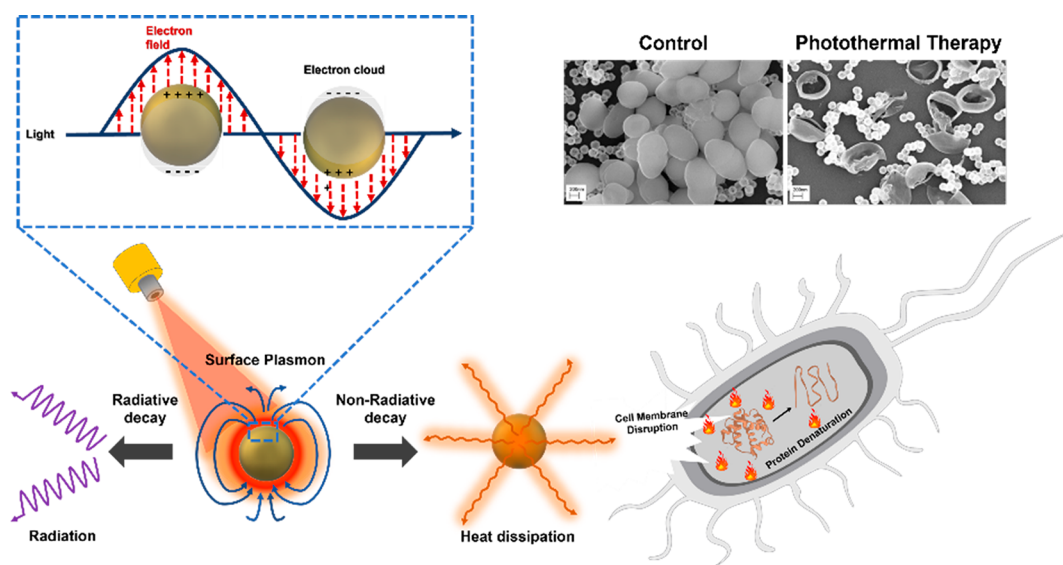


Table 1. Comparison of Photodynamic Nanomaterial–Polymer Composites for Antimicrobial Applications<sup>a</sup>

NPs	nanocomposite	particle size (nm)	PS	polymer	biomedical device	irradiation	microorganisms	treatment	CFU (log <sub>10</sub> )/antibacterial rate	ref
AuNPs	MB–NGP–PU, TBO–NGP–PU	2	MB, TBO	PU	catheter	white light of 2000 lx, 24 h irradiation	<i>S. aureus</i>	CRIs	3.8, 4.8	20
	MB–AuNPs–silicon polymer	2	MB	silicon polymer	catheter	red laser light, 155 mW, 15 min irradiation	<i>S. epidermidis</i>	CRIs	≥3	21
	MB–AuNPs–silicon polymer	2	MB	silicon polymer	catheter	light 660 nm, 250 mW laser, 10 min irradiation	<i>S. epidermidis</i> , <i>E. coli</i>	CRIs	>4, 2.2	24
	PU–AuNPs–CV	2	CV	PU	catheter	white light, ~6000 lx, 2 h irradiation	<i>S. aureus</i> , <i>E. coli</i>	CRIs	>4	23
AuAgNPs	MB–Au–PVC	2	MB	PVC	catheter	red light, 660 nm, 8 min irradiation	<i>S. epidermidis</i> , <i>E. coli</i>	CRIs		24
	RB@AuAgLNCs–PAA	40.25	RB	PAA	wound dressing	green light, 2.5 mW, 3 min irradiation	<i>Candida tropicalis</i>	wound healing		28
AgNPs	Ag/Ag@AgCl/ZnO–CMC	600		CMC	wound dressing	300 W, xenon lamp, 20 min irradiation	<i>S. aureus</i> , <i>E. coli</i>	wound healing	98.49%, 95.95%	29
	PDA/Ag <sub>3</sub> PO <sub>4</sub> /GO	10		PEEK	orthopedic implant	660 nm, 170 mW cm <sup>-2</sup> , 15 min irradiation	<i>S. aureus</i> , <i>E. coli</i>	disinfection of implant	99.66%, 99.53%	18
TiO <sub>2</sub>	G–Ag–PMMA		Helbo Blue	PMMA	denture wearers	portable light, 2000–4000 nW cm <sup>-2</sup> , 3 min irradiation	<i>P. gingivalis</i> , <i>E. faecalis</i>	halitosis and oral infections		48
	TiO <sub>2</sub> coated on PP	5–30		PP		405 nm, 10 mW cm <sup>-2</sup> , 5 min irradiation	<i>S. aureus</i> , <i>E. coli</i>	nosocomial infection		52
ZnO	CV–ZnO–PU	18.3 ± 4.9	CV	PU	antimicrobial surfaces	white-light source, 6600 ± 990 lx, 2 h irradiation	<i>S. aureus</i> , <i>E. coli</i>	nosocomial infection	99.9%	53
	CV–ZnO–silicon polymer	3–4	CV	silicon polymer	antimicrobial surfaces	28 W, white hospital light source, 3750 lx, 6 h irradiation	<i>S. aureus</i> , <i>E. coli</i>	HAI		54
	CV–ZnO–PDMS	60	CV	PDMS	antimicrobial surfaces	white light, 6500 ± 300 lx, 45 min	<i>S. aureus</i> , <i>E. coli</i>	HAI	>4	50
Cu <sub>2</sub> O	CV–ZnO–PDMS	60	CV	PDMS	antimicrobial surfaces	General Electric 28 W fluorescent lamp with a color temperature of 3500 K	<i>S. aureus</i> , <i>E. coli</i>	HAI	>4	55
	BC–SA	200		polysaccharide–SA	tooth whitening	visible GL, 60 min irradiation	<i>S. mutans</i> , <i>E. coli</i>	oral healthcare	91.15%	51

<sup>a</sup>Abbreviations: MB = methylene blue, NGP = nano gold particle, PU = polyurethane, TBO = toluidine blue, *S. aureus* = *Staphylococcus aureus*, CRIs = catheter-related infections, AuNPs = gold nanoparticles, *S. epidermidis* = *Staphylococcus epidermidis*, CV = crystal violet, AuAgNPs = gold–silver nanoparticles, PVC = poly(vinyl chloride), RB = rose bengal, PAA = poly(acrylic acid), *E. coli* = *Escherichia coli*, RB@AuAgLNCs = rose bengal-functionalized lignin gold–silver nanoconjugates, CMC = carboxymethyl cellulose, ZnO = zinc oxide, G–Ag = graphene silver nanoparticles, PEEK = poly(ether ether ketone), PMMA = poly(methyl methacrylate), PP = polypropylene, TiO<sub>2</sub> = titanium oxide, IAI = implant-associated infection, TPU = thermoplastic polyurethane, HAI = hospital-acquired infection, SA = sodium alginate, and BC–SA = Bi<sub>12</sub>O<sub>17</sub>C<sub>12</sub>–Cu<sub>2</sub>O–SA.





**Figure 3.** Schematic representation of the photothermal conversion of light to heat and the subsequent antimicrobial mechanism taking place. The top right figures display scanning electron micrographs of *E. faecalis* cells before (left) and after (right) treatment with photothermal nanomaterials. Reproduced with permission from ref 27. Copyright 2015 American Chemical Society.

antibacterial activity upon exposure to visible light. In 2017, a simple swell–encapsulate–shrink process was described as a means of achieving white-light-activated bactericidal surfaces.<sup>50</sup> The authors implanted ZnO nanoparticles with varied nanoparticle concentrations and CV into poly-(dimethylsiloxane) (PDMS) in order to create antimicrobial surfaces. ZnO/CV composites display antibacterial properties, depending on the ZnO concentration in polymer films. The ZnO/CV composite containing 0.5 g of ZnO was the most effective antibacterial polymer surface in this study, with light-activated photosensitization of *S. aureus* in 45 min and *E. coli* in 90 min, resulting in minimum of a 4 log reduction of both bacteria.<sup>50</sup> Using photodynamic dental therapy, a three-dimensional cross-linked network structure composite (BC–SA) containing a sodium alginate hydrogel membrane (SA) doped with bismuth oxychloride ( $\text{Bi}_{12}\text{O}_{17}\text{Cl}_{12}$ ) and  $\text{Cu}_2\text{O}$  nanoparticles was designed to simultaneously achieve local tooth whitening and biofilm removal.<sup>51</sup> Under green-light (GL) irradiation, this hydrogel may establish a biofilm removal coating on the target tooth surface and inhibit metabolism via ROS generated by  $\text{Bi}_{12}\text{O}_{17}\text{Cl}_{12}$  and  $\text{Cu}_2\text{O}$  nanoparticles, which is a promising strategy for oral healthcare in the future (Figure 2b).<sup>51</sup>

**2.1.3. Challenges and Future Outlooks for Antimicrobial Photodynamic Nanoparticle–Polymer Composites.** PDT candidates for antibacterial applications have shown tremendous promise. Researchers have developed photodynamic nanoparticle–polymer composites with high antibacterial efficacy against pathogenic microorganisms in biomedical devices (Table 1). While the use of PDAs has shown promise, there are obstacles that may limit this treatment’s efficacy. Despite the successful targeting of certain bacterial species in vitro, the oxygen free radicals created by these PDAs may damage mammalian cell membranes. As a result, cytotoxicity remains a key problem for implantable biomedical devices such as orthopedic implants and prostheses.<sup>14</sup> For this technology to be therapeutically effective, future attempts must include thoughtful design principles and analytical techniques before antibacterial efficacy. Importantly, materials and combinations

with conduction and valence band edges above and below the necessary ROS reaction redox potentials must be examined. Additionally, the total band gap necessary to initiate the reaction must be carefully evaluated. This should ideally remain within the biomedically significant energy levels associated with NIR-light wavelengths. Furthermore, the fabrication of Janus nanoparticles, which are formed by two or more semiconducting materials, may enable this activity to occur within a single particle, resulting in increased photodynamic characteristics.<sup>56,57</sup>

**2.2. Photothermal Antimicrobial Nanoparticle–Polymer Composites.** **2.2.1. Mechanism of Antimicrobial Photothermal Therapy (APTT).** Apart from PDT, the absorbance of light by nanomaterials can be employed to generate a rapid and significant increase in the local temperature via photothermal effects.<sup>58</sup> This process, known as PTT, was originally designed to treat cancer cells by using light-absorbing dyes. However, recent breakthroughs in nanotechnology have enabled the creation of photothermal nanoparticles capable of converting light into heat.<sup>58,59</sup> Nowadays, a broad spectrum of nanoparticles are being used in PTT. These nanoparticles are mostly noble metals (Au, Ag, and Pd), carbon-based materials, transition-metal nanostructures (e.g.,  $\text{WS}_2$  and  $\text{MoS}_2$ ), metal chalcogenides (e.g.,  $\text{Cu}_{2-x}\text{E}$ , where E = S, Se, and Te), and metal oxide nanoparticles (e.g.,  $\text{WO}_3$ ).<sup>59–62</sup> The photothermal features of these nanoparticles are caused by the resonant oscillation of the surface electrons, known as surface plasmons, or the energy of the band transition. Localized surface plasmon resonance occurs when light is irradiated onto plasmonic nanoparticles. Specifically, electrons in the conduction band at the surface of the nanomaterials are induced to oscillate and create a rapidly moving electron cloud by the electromagnetic field, as shown in Figure 3a.<sup>62,63</sup> This absorbed energy can be released by re-emission of a photon or via electron–electron interactions and electron–phonon relaxation, which causes lattice structures to vibrate and convert thermal energy to localized heat around the nanomaterials.<sup>62</sup> Thus, plasmonic nanoparticles are considered to be PTAs. For nonplasmonic nanoparticles, the

PTAs absorb light energy and undergo an electronic transition from the ground state ( $S_0$ ) to the excited singlet state ( $S_1$ ), resulting in the nonradiative relaxation of an unstable excited electron that releases kinetic energy as heat on surfaces.<sup>64</sup> The elevated temperature of both plasmonic and nonplasmonic nanomaterials through the photothermal phenomenon denatures the proteins on the bacterial surface and terminates internal processes, resulting in the death of the bacteria.<sup>65</sup> Near-infrared (NIR) light, often referred to as the “bio-transparent window” (750–900 nm), is the most suitable light source for PTT due to its ability to deeply penetrate biological tissues with low absorption by tissue chromophores such as water, hemoglobin, and melanin.<sup>66,67</sup>

**2.2.2. Photothermal Antimicrobial Nanomaterial–Polymer Composites.** The use of photothermal approaches potentially brings prospective advancements in the combat against antibiotic-resistant biofilm infections of medical devices.<sup>68</sup> Therefore, nanomaterial–polymer composite devices, which serve as models for biomedical devices such as implants,<sup>17,19</sup> catheters,<sup>23,25</sup> patches,<sup>69,70</sup> and wound dressings<sup>30,31,71,72</sup> with photothermal properties, are designed to provide antibacterial qualities, as concluded in Table 2. According to our literature research, AuNPs with various sizes and shapes are one of the most investigated nanomaterials for biomedical device sanitation.<sup>60</sup> For instance, Zhao et al. discovered that PU-conjugated gold nanorods (AuNRs) coated with poly(ethylene glycol) (PU–Au–PEG) nanocomposites were effective antimicrobial materials under NIR-light (808 nm) irradiation. In the biomedical industry, PU is commonly used to treat hernias.<sup>16</sup> AuNRs with a length of 40 nm and a width of 10 nm were immobilized on a PU surface via Au–S bonds. Additionally, thiol-modified poly(ethylene glycol) (PEG-SH), a highly hydrophilic polymer, was postmodified to generate organic/inorganic hybrid coatings (PU–Au–PEG) with intrinsic antifouling capabilities, as illustrated in Figure 4a. After irradiation with NIR light for 10 min, the temperature of PU–Au–PEG nanocomposites increased from 20 to 55 °C, demonstrating a greater photothermal efficiency than that for polymer employed alone. Confocal laser scanning microscopy images indicated the successful eradication of pathogens using 808 nm NIR light and PU–Au–PEG nanocomposites that were effective against Gram-positive (*S. aureus*) and Gram-negative (*P. aeruginosa*) bacteria. PU–Au–PEG may also prevent bacterial debris buildup in the absence of an external stimulus and inhibit the formation of biofilms due to its inherent antifouling characteristic. In general, the in vitro and in vivo antibacterial activities of hybrid nanocoatings in this work were improved by the photothermal effects of AuNRs and the hydrophilicity of PEG, making them ideal antimicrobial nanocoatings for meshes used to treat hernias.<sup>16</sup> In a recent study utilizing gold nanoshells (AuNSs) as PTAs, the Lee group reported carboxylic acid-terminated thiol-functionalized AuNSs covalently attached to amino-functionalized PDMS surfaces as model catheter surfaces and tested their effectiveness at killing *Enterococcus faecalis* bacteria (Figure 4b).<sup>27</sup> In a separate study, Hu and colleagues developed a localized heat management system for targeted antibacterial therapy that has the potential to be used in wound dressing, as shown in Figure 4c.<sup>73</sup> On the basis of the plasmonic-enhanced photothermal property, they synthesized gold nanostars with an average size of 14 nm and immobilized them with poly(*N*-isopropylacrylamide) so that they could be distributed in the depressed region of PDMS. When irradiated by NIR at a

power density of 70 mW cm<sup>-2</sup>, the average temperature of the film was maintained below 60 °C (~58 °C) at a certain concentration of AuNSs (0.2 nM). In vivo studies on *S. aureus*-infected mice revealed that films effectively eliminate infection and promote wound healing under NIR irradiation.<sup>73</sup>

Gallic acid-conjugated silver nanoparticles (GA-AgNPs; Figure 5) were discovered to have a photothermal conversion efficiency of 48.70%, making them a promising option for use against antibiotic-resistant bacteria.<sup>74</sup> With a rapid increase in the temperature and the release of silver ions, these composites demonstrated the efficient elimination of harmful disease-causing microorganisms. In an in vivo rat model, GA-AgNPs embedded in carrageenan hydrogels demonstrated enhanced wound healing with a photothermal effect in addition to increased antibacterial action with 808 nm NIR laser irradiation. The heat released by GA-AgNP hydrogels was adequate to kill pathogenic bacteria known to cause severe infections, and the heat released by these nanoparticles encouraged a quick healing effect on wounds. According to this study, up to 98.7% and 94.8% of the *E. coli* and *S. aureus* bacteria were destroyed by NIR laser irradiation at 2 W cm<sup>-2</sup> for 10 min, respectively. Similar outcomes were also shown by an in vitro bacterial culture.<sup>74</sup> The ability to obtain an efficient photon-to-heat conversion has been expanded to other metal nanoparticles. For example, copper nanoparticles (CuNPs) and copper sulfide nanoparticles (CuSNPs) have gained substantial interest for modifying wound dressing devices, due to their high redox potential, comparatively low cost to manufacture, and superior antibacterial activity against viruses, fungi, and Gram-positive and Gram-negative bacteria.<sup>75–78</sup> In a recent experiment, Ren and colleagues presented a novel strategy to prepare a photothermal antibacterial silk fabric (SF) utilizing CuSNPs. *S. aureus* and *E. coli* bacteria were killed by 99.99% within 5 min of NIR light irradiation on a composite SF. Table 2 lists the other nanoparticles that can be used for therapeutic strategies against bacterial infections, together with their application in biomedical devices.

**2.2.3. Challenges and Future Outlooks for Antimicrobial Photothermal Nanoparticle–Polymer Composites.** The antibacterial application of photothermal nanoparticles is a relatively new phenomenon, originally proven less than 2 decades ago.<sup>88</sup> There is tremendous potential for the application of this technology as a stimuli-activated antimicrobial therapeutic strategy to enhance or replace sanitation methods in biomedical devices. It possesses a spectrum of light activation in the NIR area that is capable of penetrating human cells and can combat infections in deep tissue.<sup>66,67</sup> It should be emphasized, however, that even within this biological window penetration depths are limited to a few centimeters, which may not be appropriate for broader cases of infection and implantable medical devices in the body.<sup>89,90</sup> In addition, despite the fact that therapeutic applications of PTT have achieved significant advancements, the harm to normal tissues and limited effectiveness pose ongoing challenges.<sup>91</sup> To prevent nosocomial infections, future studies should investigate the potential of this technique to design more photothermal biomedical devices rather than catheters, wound dressings, and implants. Furthermore, as human cells are extremely vulnerable to heat rises, future study should explore the range of possible photothermal treatments against fungal infections, while further in vivo investigations are needed to establish any potential harmful consequences.

Table 2. Comparison of Photothermal Nanomaterial–Polymer Composites for Antimicrobial Applications<sup>a</sup>

NPs	nanocomposite	particle size (nm)	polymer	biomedical device	irradiation	microorganisms	treatment	elevated temperature (°C)	ref
AuNPs	K/Au NHs-G	630 ± 10	polyimide	patch	980 nm, 2 W cm <sup>-2</sup> , 10 min irradiation	<i>E. coli</i> , <i>E. faecalis</i> , <i>S. epidermidis</i>	infected skin	60	69
	cellulose patch with AGE micro rods	115 ± 27	cellulose	cellulose patch	808 nm, 4 W cm <sup>-2</sup> , 20 min irradiation	<i>E. coli</i>	desalination, sterilization	264	70
	GNR/mesh	13 × 49	polypropylene	surgical meshes	810 nm, 0.435 W cm <sup>-2</sup> , 30 s irradiation	<i>S. aureus</i>	hernia repairing		79
	AuNR_mPEG-loaded glycol chitin hydrogel	29 × 105	glycol chitin hydrogel	prosthetic implant	808 nm, 1 W cm <sup>-2</sup> , 20 min irradiation	<i>S. aureus</i>	prosthetic joint infections	100	17
	TA-PEG-Au-PDMS	40 < , >70	PDMS	surgical implants	808 nm, 1.5 W cm <sup>-2</sup> , 10 min irradiation	<i>S. aureus</i> , <i>E. coli</i>	implant-associated infections	55	19
	PU-Au-PEG	10 × 40	PU	prosthetic meshes	808 nm, 1.2 W cm <sup>-2</sup> , 10 min irradiation	<i>S. aureus</i> , <i>P. aeruginosa</i>	hernia repairing	55	16
	PU-Au-QDED	10 × 40	PU	biomedical devices	808 nm, 0.8 W cm <sup>-2</sup> , 10 min irradiation	<i>S. aureus</i> , <i>E. coli</i>	antibacterial therapeutics	47	80
	PVA-GNS and PVA-Ag/GNS	GNS, 80–100; AgNPs, 8	PVA	medical device	800 nm, 0.3 W cm <sup>-2</sup> , 30 min irradiation	<i>S. aureus</i> , <i>E. coli</i>	wound disinfection or healing	52	81
	PVA-GNS	80–100	PVA	wound dressing substrates	1064 nm, 4 W cm <sup>-2</sup> , 5 min irradiation	<i>E. coli</i>	wound healing	~57	30
	E/SMM-PNAGA-Au@PDA	10 × 49	PNAGA	wound dressing	808 nm, 2 W cm <sup>-2</sup> , 5 min irradiation	<i>S. aureus</i> , <i>E. coli</i>	wound healing	65	31
	AuNS-modified PDMS	185 ± 19	PDMS	catheter	810 nm, 2.5 W cm <sup>-2</sup> , 10 min irradiation	<i>E. faecalis</i>	CRIs	73	27
	AuNS-PDMS-pNIPAM	14	PDMS-pNIPAM	TRIM films	NIR irradiation, 70 m W cm <sup>-2</sup> , 8 min	<i>E. coli</i> , <i>P. aeruginosa</i> , <i>S. aureus</i>	antibacterial therapy	58	73
	HAuNS-containing patch	116.7 ± 15.3	cellulose	sterilization patches	808 nm, 4 W cm <sup>-2</sup> , 10 min irradiation	<i>E. coli</i>	wound healing	63	32
	Au@CuS/PDMS	195.1 ± 21.4	PDMS	biomedical devices	808 nm, 3.5 W cm <sup>-2</sup> , 10 min irradiation	<i>E. coli</i>	sterilization	210	81
AgNPs	GA-AgNP hydrogel	43	polysaccharide-carrageenan	antibacterial hydrogel	in vitro (808 nm, 1.5 W cm <sup>-2</sup> , 10 min), in vivo (808 nm, 1.5 W cm <sup>-2</sup> , 2 min)	<i>S. aureus</i> , <i>E. coli</i>	wound healing	in vitro (bacterial survival ratios of 1.3% for <i>E. coli</i> and 5.2% for <i>S. aureus</i> ), in vivo (30.6)	74
	Ag/SiO <sub>2</sub> NPs	10–14	PDMS	medical devices	808 nm, 1.4 W cm <sup>-2</sup> , 10 min irradiation	<i>S. aureus</i> , <i>E. coli</i>	medical-device-related infections	68	82
	GLASS-PEI-TRI	120 ± 25	PEI	surgical and prosthetic surfaces	808 nm, 0.26 W cm <sup>-2</sup> , 15 min irradiation	<i>S. aureus</i> , <i>E. coli</i>	medical-device-related infections	~37	15
	AgNPs@EL	20	lignin	wound dressing	808 nm, 1.8 W cm <sup>-2</sup> , 5 min irradiation	<i>S. aureus</i> , <i>E. coli</i>	wound healing	55	83
	AgSLS/PPy-PDA@-PEGDA hydrogel	220	PEGDA	wound dressing	808 nm, 2 W cm <sup>-2</sup> , 3 min irradiation	<i>S. aureus</i> , <i>E. coli</i>	wound healing	52.9	84
	CuSNPs-HA-Fe <sup>3+</sup> -EDTA hydrogel	~70	hyaluronic acid	band-aid	808 nm, 0.5 W cm <sup>-2</sup> , 2 min irradiation	<i>S. aureus</i>	wound healing	41–45	85
	BACA/CuNP/Gel-MA hydrogel	110	Gel-MA	therapeutic dressing	808 nm, 1.2 W cm <sup>-2</sup> , 10 min irradiation	<i>S. aureus</i> , <i>E. coli</i>	wound healing	42	76
CuNPs	CuNP-deposited SF	20–50	QCS	antibacterial SF	808 nm, 0.4 W cm <sup>-2</sup> , 5 min irradiation	<i>S. aureus</i> , <i>E. coli</i>	antibacterial materials	102	77
Fe <sub>3</sub> O <sub>4</sub> NPs	Fe <sub>3</sub> O <sub>4</sub> @PDMS	360 ± 10	PDMS	catheter	808 nm, 1 W cm <sup>-2</sup> , 10 min Irradiation	<i>S. aureus</i> , <i>E. coli</i>	CRIs	100	25
Bi <sub>2</sub> S <sub>3</sub> NPs	Bi <sub>2</sub> S <sub>3</sub> NPs hydrogel	200	SA-acrylamide hydrogels	wound dressing	808 nm, 2 W cm <sup>-2</sup> , 10 min irradiation	<i>S. aureus</i> , <i>E. coli</i>	wound healing	57	86



Table 2. continued

NPs	nanocomposite	particle size (nm)	polymer	biomedical device	irradiation	microorganisms	treatment	elevated temperature (°C)	ref
MCS nano-wires	MCSA	10–100	polysaccharide–SA	wound dressing	in vitro (808 nm, 2.6 W cm <sup>-2</sup> , 15 min), in vivo (808 nm, 1.8 W cm <sup>-2</sup> , 15 min)	B16F10	wound healing	in vitro (viability of cells: 10.6% for B16F10) in vivo (55 °C, tumor growth was suppressed)	72
MoS <sub>2</sub> nano-clusters	SA–MS hydrogel	300–400	polysaccharide–SA	wound dressing	in vitro (808 nm, 0.6 W cm <sup>-2</sup> , 10 min), in vivo (808 nm, 0.6 W cm <sup>-2</sup> , 10 min)	B16F10	wound healing		87

<sup>a</sup>Abbreviations: Au NHs = gold nanoholes, K/Au NHs = gold nanohole-modified kapton, K/Au NHs-G = graphene-coated gold nanohole-modified kapton, *E. faecalis* = *Enterococcus faecalis*, *S. epidermidis* = *Staphylococcus epidermidis*, *E. coli* = *Escherichia coli*, AGE = armored golden *E. coli*, GNR = gold nanorod, AuNR\_mPEG = PEGylated gold nanorods, TA = tannic acid, PEG = poly(ethylene glycol), PDMS = poly(dimethylsiloxane), PU = polyurethane, QDED = quaternized N,N'-dimethylethylenediamine, GNS = gold nanostar, PVA = poly(vinyl alcohol), Ch/AuNRs = chitosan-based hydrogel embedded with gold nanorods, E/SMM = *E. coli*- or *S. aureus*-pretreated macrophage membrane, PNAGA = poly(N-acryloylglycinamide), CRLs = catheter-related infections, *B. subtilis* = *Bacillus subtilis*, MRSa = methicillin-resistant *Staphylococcus aureus*, *P. aeruginosa* = *Pseudomonas aeruginosa*, *A. baumannii* = *Acinetobacter baumannii*, GO = graphene oxide, TRIM = thermal-disrupting interface-induced mitigation, AuNS = gold nanostar, pNIPAM = poly(N-isopropylacrylamide), HAuNS = hollow gold nanospheres, GA-AgNPs = gallic acid-functionalized silver nanoparticles, *S. aureus* = *Staphylococcus aureus*, PEI = polyethylenimine, TRI = triangle gold nanoplate, AgNPs@EL = lignin-based nanosilver composites, EL = extracted lignin, Ag-SLS NPs = silver sodium lignin sulfonate nanoparticles, PEGDA = poly(ethylene glycol diacrylate), Gel-MA = methacrylated gelatin, BACA = N,N'-bis(acryloyl)cystamine, QCS = chitosan quaternary ammonium salt, SF = silk fabric, Bi<sub>2</sub>S<sub>3</sub> NPs = bismuth sulfide nanoparticles, SA = sodium alginate, MCSA = manganese-doped calcium silicate nanowires alginate hydrogel, MCS = manganese-doped calcium silicate, MoS<sub>2</sub> = molybdenum disulfide, and MoS<sub>2</sub>-Van-FITC@CS = fluorescein 5(6)-isothiocyanate (FITC)-labeled and Van-loaded MoS<sub>2</sub>-nanosheet hydrogels.

**2.3. Dual Synergistic Antimicrobial-Based PDT/PTT Nanoparticle–Polymer Composites.** **2.3.1. Mechanism of Dual Synergistic Antimicrobial-Based PDT/PTT.** In recent years, dual synergistic photoactivated therapies (PDT/PTT) have attracted considerable interest as antibacterial alternative treatments due to their high therapeutic efficacy, noninvasive nature, and fewer side effects than conventional therapeutic systems (Table 3).<sup>92–96</sup> PTT employs photothermal transducing agents to transform light energy into heat energy for bacterial eradication; it offers remote control capability, minimal invasiveness, rapid treatment, and deep-tissue penetration. However, a higher temperature (over 70 °C) is required to achieve antibacterial effectiveness for single PTT, which would scald normal tissues and cause serious side effects.<sup>92</sup> Differently, PDT utilizes a light source to activate PS and generate ROS to kill target bacteria with less damage to host cells, making it safer.<sup>58,92</sup> PDT is also reusable and practical for treating infectious diseases, but its antibacterial applicability in deep tissue and ROS production is limited by the photochemical characteristics of PS and the ability of the excitation light source to penetrate biological tissues.<sup>58</sup> The formation of ROS is closely related to the energy of light. Long-wavelength light has little influence on the promotion of PDT because it lacks the energy to generate ROS.<sup>97,98</sup> UV light is often utilized in PDT and is effective at killing microorganisms, yet it can harm DNA and biological tissue. The use of visible light with long wavelengths and NIR light in PTT, on the other hand, is less damaging to tissues.<sup>6</sup> Another concern is that a large amount of ROS is necessary to kill the majority of bacteria with a single PDT. However, during this process, high levels of ROS caused damage to surrounding normal tissues, including inflammation, fibrosis, and even necrosis, during this phase.<sup>58</sup> Therefore, the development of dual phototherapy strategies is of the utmost importance for tissue-compatible antibacterial treatment.

These strategies should include PTT with a lower temperature (about 50 °C) and moderate PDT with fewer ROS during the therapeutic phase. Thus, the combination of PTT and PDT could greatly boost antibacterial efficacy through a synergistic effect while simultaneously lowering the negative effects of a single-mode antibacterial method. Researchers have observed that bacteria and biofilms harmed by photothermal impacts are more vulnerable to ROS. This suggests a potential relationship between the photothermal impacts and increased susceptibility to ROS. The mechanism of these dual systems has not been explored independently. Further research is needed to fully understand the underlying mechanisms of the relationship between the photothermal impacts and vulnerability to ROS. It is believed that the heat produced by the photothermal effect could accelerate the permeability of bacteria, hence facilitating the uptake of PS and ultimately PDT.<sup>93</sup> In turn, PS-generated ROS can reduce bacteria's heat resistance, increasing the effectiveness of PTT.<sup>92,93</sup> Consequently, the synergy of PDT and PTT has the ability to overcome their individual drawbacks, thus endowing the material with greater benefits for increased antibacterial therapy. The mild heating temperature of PTT may limit the bacterial activity, making cells more susceptible to PDT disruption.<sup>58,93,108</sup>

**2.3.2. Dual Synergistic PDT/PTT Antibacterial Nanoparticle–Polymer Composites.** Dual-model light-assisted (PDT/PTT) antibacterial therapies have received significant attention in recent years due to their excellent bactericidal

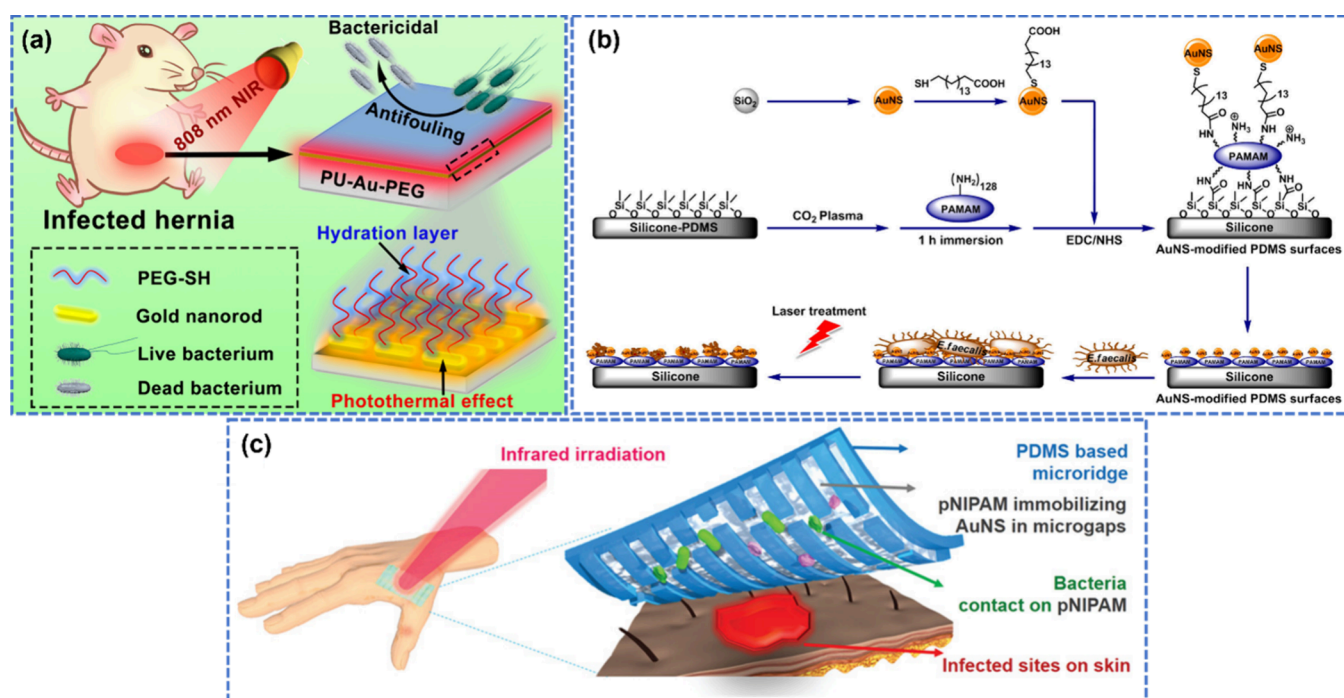


**Figure 4.** (a) Illustration of a NIR-responsive PU–Au–PEG surface with antifouling and photothermal antibacterial characteristics. Reproduced with permission from ref 16. Copyright 2020 American Chemical Society. (b) Strategy for developing AuNS-modified PDMS surfaces and evaluation of their effectiveness against *E. faecalis* under NIR illumination. Adapted with permission from ref 27. Copyright 2015 American Chemical Society. (c) Representation of a TRIM film attached to the skin that absorbs IR light and generates local heat, which kills bacteria in the depressed regions of the film while leaving the surrounding epithelial host cells unharmed. Adapted with permission from ref 73. Copyright 2020 Wiley.

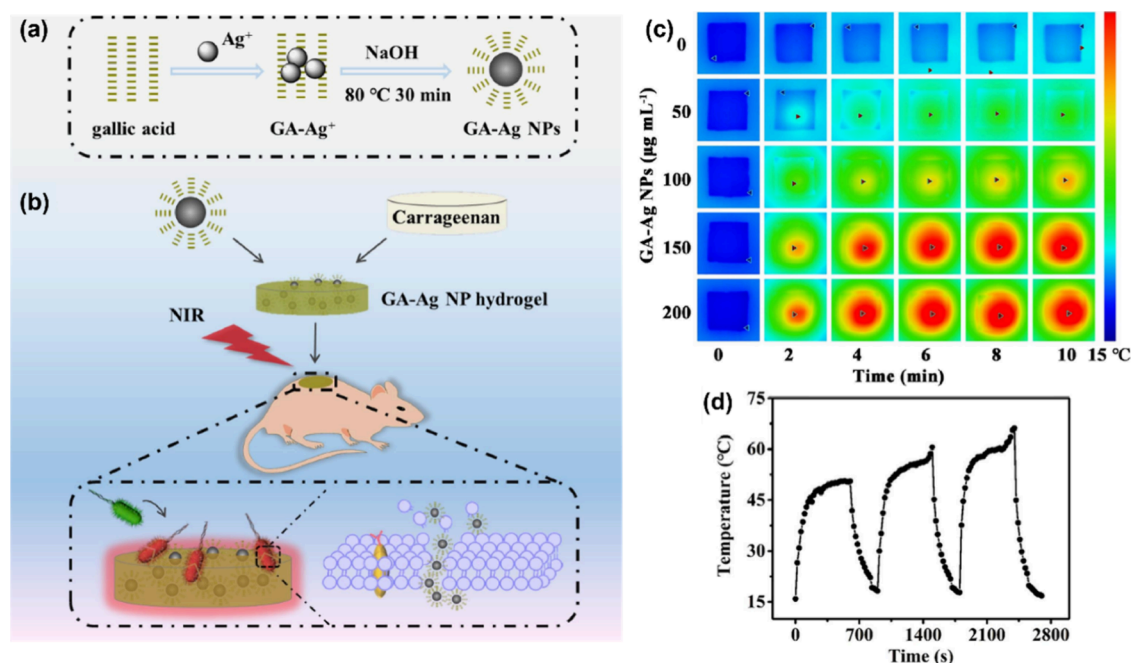


**Figure 5.** (a) Schematic of the GA-AgNPs synthesis process. (b) Illustration of GA-AgNP hydrogel composites for photothermal bacteria elimination. (c) NIR-irradiated thermal IR pictures of GA-AgNP hydrogels. (d) Increase in the hydrogel temperature across three laser on/off cycles. A laser with a wavelength of 808 nm and a power density of  $1.5 \text{ W cm}^{-2}$  was used. Reproduced with permission from ref 74. Copyright 2020 Elsevier.

efficacy and low side effects.<sup>109,110</sup> However, the implementation of these dual systems in biomedical devices is still limited. Table 3 provides a complete summary of the current status of PDT/PTT antimicrobial synergistic strategies including nano-

composites, irradiation methods, biomedical devices, and tested microorganisms. The researchers Feng et al. explored the synergistic photodynamic and photothermal properties of chitosan-assisted  $\text{MoS}_2$  ( $\text{CS@MoS}_2$ ) hybrid coatings.<sup>104</sup> They

Table 3. Comparison of PDT/PTT Nanomaterial–Polymer Composites for Antimicrobial Applications<sup>a</sup>

NPs	nanocomposite	nanoparticle size (nm)	polymer	biomedical device	irradiation	microorganisms	treatment	CFU (log <sub>10</sub> )/antibacterial rate	ref
AuNPs	Au-GO-NH <sub>2</sub> coating on PDMS	1.4 ± 0.4	PDMS	catheter	visible light, 200 mW cm <sup>-2</sup> , 10 min irradiation,	<i>S. aureus</i> , <i>E. coli</i>	antibacterial therapeutics	>99.9, >99.9	26
AgNPs	PLLA/Dex/Ag fibers		PLLA	orthopedic screws	808 nm, 1.5 W cm <sup>-2</sup> , 10 min irradiation	<i>S. aureus</i> , <i>E. coli</i>	wound disinfection	100, 97.2, 99.94	99
	Ag <sub>3</sub> PO <sub>4</sub> /MoS <sub>2</sub> /HD	10–30	PVA	wound dressing	660 and 808 nm, 0.6 W cm <sup>-2</sup> , 5 min irradiation	<i>S. aureus</i>	wound healing	99.9	100
CuNPs	CuS/mSiO <sub>2</sub> hydrogel	25	NIPAAm	wound dressing	808 nm, 2 W cm <sup>-2</sup> , 10 min irradiation	<i>S. aureus</i> , <i>E. coli</i>	wound healing	99.80, 99.94	101
	CuFe <sub>2</sub> O <sub>4</sub> /PEEK	100–150	PEEK	orthopedic implant	808 nm, 1 W cm <sup>-2</sup> , 10 min irradiation	<i>S. aureus</i> , <i>E. coli</i>	IAI	99.57	102
	LS-CuS@PVA		PVA	wound dressing	808 nm, 1.3 W cm <sup>-2</sup> , 10 min irradiation	<i>S. aureus</i> , <i>E. coli</i>	wound healing	4.8	103
MOS <sub>2</sub>	SF/PANI/CuS@PDMS		PANI	antibacterial textile	0.1–0.2 W cm <sup>-2</sup> , 5 min irradiation	<i>S. aureus</i> , <i>E. coli</i>		99.99, 99.99	78
	CS@MoS <sub>2</sub>	50–300	polysaccharide–chitosan	artificial implant	660 nm visible light, 808 nm NIR, 10 min irradiation	<i>S. aureus</i> , <i>E. coli</i>	infection prevention	99.65, 99.84	104
	MOS <sub>2</sub> /PDA–RGD	260	PDA	implant	808 nm, 0.5 W cm <sup>-2</sup> , 8 min irradiation	<i>S. aureus</i> , <i>E. coli</i>	infection prevention	92.6, 92.6	105
	CS@MoS <sub>2</sub>		PVA	wound dressing	660 nm visible light, 808 nm NIR, 0.2 W cm <sup>-2</sup> , 15 min irradiation	<i>S. aureus</i> , <i>E. coli</i>	wound healing	99.5, 99.3	106
TiO <sub>2</sub>	UCNPs@TiO <sub>2</sub> @GO		PVDF	wound dressing	980 nm, 2.5 W cm <sup>-2</sup> , 10 min irradiation	<i>S. aureus</i> , <i>E. coli</i>	wound healing	59.7	107

<sup>a</sup>Abbreviations: AuNPs = gold nanoparticles, Au-GO-NH<sub>2</sub> = gold nanoclusters-decorated amine-functionalized graphene oxide, PDMS = poly(dimethylsiloxane), AgNPs = silver nanoparticles, Dex = dexamethasone, PLLA = poly(L-lactic acid), PVA = poly(vinyl alcohol), PEEK = poly(ether ether ketone), NIPAAm = N-isopropylacrylamide, CuS = copper sulfide, NIPAAm = N-isopropylacrylamide, LS-CuS = lignin copper sulfide, SF = silk fabric, MOS<sub>2</sub>/PDA–RGD = molybdenum disulfide/polydopamine–arginine–glycine–aspartic acid, PDA = polydopamine–arginine, IAI = implant-associated infection, PVDF = poly(vinylidene fluoride), GO = graphene oxide, UCNPs = upconversion nanoparticles, and PANI = polyaniline.

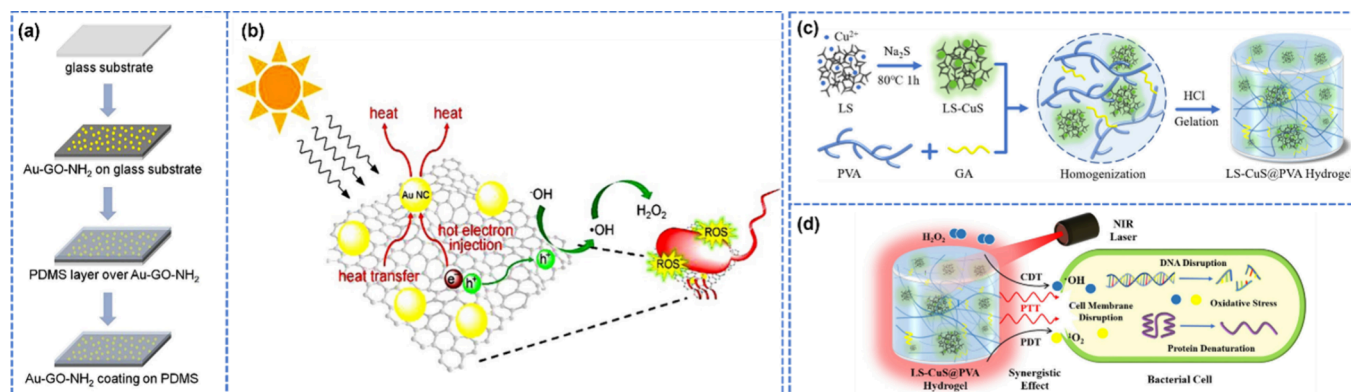


**Figure 6.** (a) Illustration of the coating of Au-GO-NH<sub>2</sub> nanosheets on the surface of silicone. (b) Representation of the antibacterial process of Au-GO-NH<sub>2</sub> nanosheets upon exposure to visible light. Reproduced with permission from ref 26. Copyright 2020 Elsevier. (c) Schematic diagram of the LS-CuS@PVA composite hydrogel preparation process. (d) Diagrams depicting the synergistic antibacterial mechanism of LS-CuS@PVA. Adapted with permission from ref 103. Copyright 2022 American Chemical Society.

discovered that metallic titanium implants in vivo possessed a good surface self-inhibiting ability. Under visible-light irradiation, the coating produces singlet oxygen and NIR light promotes a rise in the implant temperature. This combination produces a synergistic effect of photodynamic and photothermal effects that significantly increases the killing efficiency of *E. coli* and *S. aureus*. The incorporation of chitosan not only makes the implant more biocompatible but also offers a straightforward, fast, and risk-free method for the eradication of germs that are already present in vivo in situ.<sup>104</sup> As a potent visible-light-active antibacterial agent, Li and colleagues produced a new nanocomposite of gold nanoclusters

(AuNCs)-decorated amine-functionalized graphene oxide (Au-GO-NH<sub>2</sub>) nanosheets, as illustrated in Figure 6a,b.<sup>26</sup> This nanosheet is capable of capturing microorganisms due to physical adsorption and electrostatic contact. Under visible light, this photoactive nanosheet generates considerable heat and high ROS. This nanosheet is 5 times more bactericidal against Gram-positive and Gram-negative bacteria than AuNCs and amine-functionalized GO. A nanosheet-modified silicone surface was also employed as a model for implant devices, displaying antibacterial effectiveness against in vitro bacterial colonization. The generated nanosheet can be used to develop the next generation of antimicrobial medications for



biomedical and environmental applications using synergistic bacterial capture, oxidative stress, and photothermal ablation.<sup>26</sup>

CuSNPs are frequently utilized as dual synergistic antibacterial systems due to their distinctive semiconducting properties and photothermal conversion efficiency.<sup>78,101,103</sup> The Xie group has recently introduced lignin copper sulfide (LS-CuS) nanocomposites that are incorporated into a poly(vinyl alcohol) (PVA) hydrogel to create an LS-CuS@PVA composite hydrogel with NIR-activated photothermal, photodynamic, and peroxidase-like performances for wound healing and wound dressing (Figure 6b).<sup>103</sup> In the presence of H<sub>2</sub>O<sub>2</sub> and NIR light for 10 min, LS-CuS@PVA displayed the high antibacterial rate with 3.8-log and 4.8-log reductions of colony-forming units (CFUs) against *E. coli* and *S. aureus*, respectively. Due to the combined action of hyperthermia and ROS, the antibacterial activity of the LS-CuS@PVA system was considerably strengthened, and the LS-CuS@PVA hydrogel can eliminate bacteria that have already grown and inhibit their creation.<sup>103</sup> The Li group synthesized another hybrid nanocomposite consisting of 3-(trimethoxysilyl)propyl methacrylate (97%) and mesoporous silica (mSiO<sub>2</sub>) modified CuSNPs.<sup>101</sup> This nanocomposite exhibits outstanding and controllable photothermal and photodynamic characteristics under 808 nm NIR irradiation as well as antibacterial activity of 99.80% and 99.94% against *S. aureus* and *E. coli*, respectively, within 10 min. In addition, the release of copper ion during NIR irradiation leads to antimicrobial action and skin tissue generation.<sup>101</sup> In 2023, a new study reported the development of photothermal and photodynamic antimicrobial fabrics.<sup>78</sup> Because SFs contained few chelating sites (carboxyl, hydroxyl, and amino groups) on their own, polyaniline (PANI) was added to fiber surfaces to chelate copper ammonia ions and facilitate CuSNP deposition. Copper ammonia ions were coupled to SF/PANI and interacted with thiourea adsorbed on the chitosan quaternary ammonium salt template to distribute CuSNPs uniformly on the fiber surface and increase the specific surface area. The photothermal textile was finally encapsulated with PDMS, which provided antioxidant and self-cleaning properties. The results indicated that the UV resistance of the SF/PANI/CuS composite textile was satisfactory. The inactivation of *S. aureus* and *E. coli* reached 99.9% after 5 min of irradiation at 200 mW cm<sup>-2</sup> and remained at the same level after 10 washings.<sup>78</sup>

**2.3.3. Challenges and Future Outlooks for Dual Synergistic PDT/PTT Antimicrobial Nanoparticle–Polymer Composites.** The synergistic antibacterial method of PDT/PTT has a greater potential to eradicate bacteria than PTT and PDT alone, due to the PTT process' ability to increase temperature appropriately, thereby increasing the permeability of the cell membrane by enzyme denaturation and damaging the protein and phospholipids on the cell membrane, making bacteria more susceptible to ROS damage and achieving significantly improved antibacterial efficacy.<sup>111</sup> However, the design of such dual-mode antimicrobial agents has obstacles, such as the necessity to combine multiple compounds, which results in complex synthesis processes and biocompatibility concerns.<sup>93,112</sup> The intricate interplay between various components within hybrid materials may pose challenges in achieving optimal synergistic effects. Addressing this concern requires a meticulous investigation into the selection of constituents, their ratios, and potential modifications to streamline the synthesis while ensuring the safety and biocompatibility of the resulting composites. In addition,

hybrid materials containing several chemicals may be influenced by the requirement for two light sources to generate the superposition of the two therapeutic actions, which enhances the laser exposure time.<sup>93,113</sup> This approach presents a practical challenge in achieving optimal treatment outcomes while minimizing the potential side effects. Future research endeavors should focus on the development of innovative materials that can harness the benefits of dual-mode therapy with a single light source, reducing complexity and enhancing the clinical feasibility of the approach. Furthermore, the safety of long-term use in the human body and the therapeutic application in the human body must be evaluated, particularly for implantable biomedical devices.<sup>6,114</sup> The intensity and controllability of the produced immune response were also taken into account. Understanding the interaction between advanced materials and the complex biological environment is crucial for ensuring sustained efficacy without adverse effects. Future studies should delve into long-term in vivo assessments, considering factors such as material degradation, immune responses, and overall biocompatibility, to pave the way for the practical implementation of these technologies in therapeutic application. Consequently, despite the fact that phototherapy based on nanoparticles and a combination treatment has been actively researched, many projects are still in the discovery phase, and there are still a great number of shortcomings that must be addressed.

### 3. CONCLUSIONS AND FUTURE PERSPECTIVES

Humans are endangered by the rising resistance to pathogenic microorganisms. Because new antibiotics cannot keep up with the evolution of pathogen resistance, numerous efforts have been made to develop alternative antibacterial strategies to tackle MDR bacteria. Importantly, the discovery and development of light-stimulated antimicrobial nanomaterials offer a possible solution to combating the worldwide nosocomial infection problem and are promising alternatives.<sup>12,13</sup> The application of PTT and PDT for combating nosocomial infections is still in the experimental stage and is not yet widely used in clinical practice. However, there have been some studies that have shown promising results using these therapies to kill pathogenic bacteria and fungi responsible for nosocomial infections.

Photodynamic nanomaterial agents are among the most extensively studied light-activated treatments for pathogenic microbes, and they demonstrate extraordinary antimicrobial activity.<sup>34</sup> This technology faces challenges to reduce cytotoxicity and treatment time, as well as to modify important factors, such as the size and composition of the nanomaterial, the need to shift the excitation wavelength into the NIR region, which is demanded for clinical applications, while providing sufficient redox potential to boost the generation of antimicrobial ROS.<sup>14</sup> Comparatively, PTAs that induce localized hyperthermia as a consequence of exposure to light show promise in the treatment of nosocomial infections because they can be activated by NIR wavelengths through biological windows, to which human tissue is highly permeable, and can therefore penetrate human tissue.<sup>58</sup> However, penetration depths are still limited to a few centimeters, and damaging normal tissues as the temperature rises remains a challenge.<sup>90</sup> Consequently, these technologies are still in the developmental stage, and future research will require systematic studies and in vivo trials. Another important strategy is the development of dual-model light-assisted (PDT/PTT) anti-

bacterial therapies, which are more effective at eliminating bacteria than PTT and PDT alone.<sup>92</sup> The ability of PTT to appropriately raise the temperature increases the permeability of the cell membrane by enzyme denaturation and damages the cell membrane proteins and phospholipids, making bacteria more susceptible to ROS damage and enhancing antibacterial efficacy.<sup>111</sup> However, there are still concerns surrounding the complexity of developing dual systems, their safety, and laser exposure duration. Numerous initiatives are still in the exploration stage, and difficulties must be overcome.<sup>114</sup>

Overall, this paper summarizes the most recent developments in photostimulated-responsive nanomaterials and their cutting-edge applications in antibacterial properties of biomedical devices, as well as their significance in the field of healthcare. This review also addresses the limitations of these technologies, which require additional systematic investigations and in vivo trials to optimize and evaluate their “real world” applicability. It is important to note that these therapies are still in the early stages of development, and further research is needed to determine their safety and efficacy in the treatment of nosocomial infections. The limitations highlighted in this review act as guideposts for future research, urging the scientific community to delve deeper into the intricacies of these emerging therapies. The early stages of development underscore the imperative for amplified research efforts to determine the safety, efficacy, and practical viability of these innovative approaches in the intricate landscape of nosocomial infection treatment. In essence, the latest advancements not only showcase the potential of light-stimulated antimicrobial nanomaterials, but also advocate for a collaborative effort to address the challenges and propel these technologies from promising concepts to impactful solutions in the field of healthcare.

## AUTHOR INFORMATION

### Corresponding Author

**T. Randall Lee** – Department of Chemistry and Texas Center for Superconductivity, University of Houston, Houston, Texas 77204, United States; [orcid.org/0000-0001-9584-8861](https://orcid.org/0000-0001-9584-8861); Email: [trlee@uh.edu](mailto:trlee@uh.edu)

### Authors

**Mina Omidian** – Department of Chemistry and Texas Center for Superconductivity, University of Houston, Houston, Texas 77204, United States; [orcid.org/0000-0002-5017-5269](https://orcid.org/0000-0002-5017-5269)

**Pannaree Srinoi** – Department of Chemistry, Faculty of Science, Kasetsart University, Bangkok 10900, Thailand; [orcid.org/0000-0003-4400-468X](https://orcid.org/0000-0003-4400-468X)

**Pooria Tajalli** – Department of Chemistry and Texas Center for Superconductivity, University of Houston, Houston, Texas 77204, United States; [orcid.org/0000-0001-7415-0587](https://orcid.org/0000-0001-7415-0587)

Complete contact information is available at: <https://pubs.acs.org/10.1021/acsnm.3c05173>

### Notes

The authors declare no competing financial interest.

## ACKNOWLEDGMENTS

The Air Force Office of Scientific Research (AFOSR FA9550-23-1-0581; 23RT0567) and the Robert A. Welch Foundation (Grant E-1320) generously supported this research.

## REFERENCES

- (1) Ananda, T.; Modi, A.; Chakraborty, I.; Managuli, V.; Mukhopadhyay, C.; Mazumder, N. Nosocomial Infections and Role of Nanotechnology. *Bioengineering* **2022**, *9*, 51.
- (2) Haque, M.; Sartelli, M.; McKimm, J.; Abu Bakar, M. B. Health Care-Associated Infections-an Overview. *Infect. Drug Resist.* **2018**, *11*, 2321.
- (3) Pahlevanzadeh, F.; Setayeshmehr, M.; Bakhsheshi-Rad, H. R.; Emadi, R.; Kharaziha, M.; Poursamar, S. A.; Ismail, A. F.; Sharif, S.; Chen, X.; Berto, F. A Review on Antibacterial Biomaterials in Biomedical Applications: From Materials Perspective to Bioprinting. *Polymers* **2022**, *14*, 2238.
- (4) Parham, S.; Kharazi, A. Z.; Bakhsheshi-Rad, H. R.; Kharaziha, M.; Ismail, A. F.; Sharif, S.; Razzaghi, M.; RamaKrishna, S.; Berto, F. Antimicrobial Synthetic and Natural Polymeric Nanofibers as Wound Dressing: A Review. *Adv. Eng. Mater.* **2022**, *24*, 2101460.
- (5) Nagaraj, K.; Sudhir, D. Outcome of Nosocomial Infections in the Pediatric Intensive Care Unit. *Eur. J. Mol. Clin. Med.* **2022**, *9*, 2195–2201.
- (6) Zhao, Y.; Chen, L.; Wang, Y.; Song, X.; Li, K.; Yan, X.; Yu, L.; He, Z. Nanomaterial-Based Strategies in Antimicrobial Applications: Progress and Perspectives. *Nano Res.* **2021**, *14*, 4417–4441.
- (7) Mutalik, C.; Wang, D.-Y.; Krisnawati, D. I.; Jazidie, A.; Yougbare, S.; Kuo, T.-R. Light-Activated Heterostructured Nanomaterials for Antibacterial Applications. *Nanomaterials* **2020**, *10*, 643.
- (8) Garland, M.; Loscher, S.; Bogoy, M. Chemical Strategies to Target Bacterial Virulence. *Chem. Rev.* **2017**, *117*, 4422–4461.
- (9) Willyard, C. Drug-Resistant Bacteria Ranked. *Nature* **2017**, *543*, 15.
- (10) O'Neill, J. Tackling Drug-Resistant Infections Globally: Final Report and Recommendations. *Review on Antimicrobial Resistance*; Wellcome Trust, 2016.
- (11) Makabenta, J. M. V.; Nabawy, A.; Li, C.-H.; Schmidt-Malan, S.; Patel, R.; Rotello, V. M. Nanomaterial-Based Therapeutics for Antibiotic-Resistant Bacterial Infections. *Nat. Rev. Microbiol.* **2021**, *19*, 23–36.
- (12) Han, Q.; Lau, J. W.; Do, T. C.; Zhang, Z.; Xing, B. Near-Infrared Light Brightens Bacterial Disinfection: Recent Progress and Perspectives. *ACS Appl. Bio Mater.* **2021**, *4*, 3937–3961.
- (13) Liu, S.; Li, X.; Han, L. Recent Developments in Stimuli-responsive Hydrogels for Biomedical Applications. *Biosurface Biotribology* **2022**, *8*, 290–306.
- (14) Cheeseman, S.; Christofferson, A. J.; Kariuki, R.; Cozzolino, D.; Daeneke, T.; Crawford, R. J.; Truong, V. K.; Chapman, J.; Elbourne, A. Antimicrobial Metal Nanomaterials: From Passive to Stimuli-activated Applications. *Adv. Sci.* **2020**, *7*, 1902913.
- (15) D'Agostino, A.; Taglietti, A.; Desando, R.; Bini, M.; Patrini, M.; Dacarro, G.; Cucca, L.; Pallavicini, P.; Grisoli, P. Bulk Surfaces Coated with Triangular Silver Nanoplates: Antibacterial Action Based on Silver Release and Photo-Thermal Effect. *Nanomaterials* **2017**, *7*, 7.
- (16) Zhao, Y.-Q.; Sun, Y.; Zhang, Y.; Ding, X.; Zhao, N.; Yu, B.; Zhao, H.; Duan, S.; Xu, F.-J. Well-Defined Gold Nanorod/Polymer Hybrid Coating with Inherent Antifouling and Photothermal Bactericidal Properties for Treating an Infected Hernia. *ACS Nano* **2020**, *14*, 2265–2275.
- (17) Wickramasinghe, S.; Ju, M.; Milbrandt, N. B.; Tsai, Y. H.; Navarreto-Lugo, M.; Visperas, A.; Klika, A.; Barsoum, W.; Higuera-Rueda, C. A.; Samia, A. C. S. Photoactivated Gold Nanorod Hydrogel Composite Containing D-Amino Acids for the Complete Eradication of Bacterial Biofilms on Metal Alloy Implant Materials. *ACS Appl. Nano Mater.* **2020**, *3*, 5862–5873.
- (18) Xie, X.; Mao, C.; Liu, X.; Tan, L.; Cui, Z.; Yang, X.; Zhu, S.; Li, Z.; Yuan, X.; Zheng, Y.; Yeung, K. W. K.; Chu, P. K.; Wu, S. Tuning the Bandgap of Photo-Sensitive Polydopamine/Ag<sub>3</sub>PO<sub>4</sub>/Graphene Oxide Coating for Rapid, Noninvasive Disinfection of Implants. *ACS Cent. Sci.* **2018**, *4*, 724–738.
- (19) He, X.; Sathishkumar, G.; Gopinath, K.; Zhang, K.; Lu, Z.; Li, C.; Kang, E.-T.; Xu, L. One-Step Self-Assembly of Biogenic Au NPs/

- PEG-Based Universal Coatings for Antifouling and Photothermal Killing of Bacterial Pathogens. *Chem. Eng. J.* **2021**, *421*, 130005.
- (20) Naik, A. J. T.; Ismail, S.; Kay, C.; Wilson, M.; Parkin, I. P. Antimicrobial Activity of Polyurethane Embedded with Methylene Blue, Toluidene Blue and Gold Nanoparticles against *Staphylococcus Aureus*; Illuminated with White Light. *Mater. Chem. Phys.* **2011**, *129*, 446–450.
- (21) Bovis, M. J.; Noimark, S.; Woodhams, J. H.; Kay, C. W. M.; Weiner, J.; Peveler, W. J.; Correia, A.; Wilson, M.; Allan, E.; Parkin, I. P.; MacRobert, A. J. Photosensitisation Studies of Silicone Polymer Doped with Methylene Blue and Nanogold for Antimicrobial Applications. *RSC Adv.* **2015**, *5*, 54830–54842.
- (22) Perni, S.; Piccirillo, C.; Kafizas, A.; Uppal, M.; Pratten, J.; Wilson, M.; Parkin, I. P. Antibacterial Activity of Light-Activated Silicone Containing Methylene Blue and Gold Nanoparticles of Different Sizes. *J. Clust. Sci.* **2010**, *21*, 427–438.
- (23) Macdonald, T. J.; Wu, K.; Sehmi, S. K.; Noimark, S.; Peveler, W. J.; du Toit, H.; Voelcker, N. H.; Allan, E.; MacRobert, A. J.; Gavrilidis, A.; Parkin, I. P. Thiol-Capped Gold Nanoparticles Swell-Encapsulated into Polyurethane as Powerful Antibacterial Surfaces Under Dark and Light Conditions. *Sci. Rep.* **2016**, *6*, 39272.
- (24) Noimark, S.; Dunnill, C. W.; Kay, C. W. M.; Perni, S.; Prokopovich, P.; Ismail, S.; Wilson, M.; Parkin, I. P. Incorporation of Methylene Blue and Nanogold into Polyvinyl Chloride Catheters; a New Approach for Light-Activated Disinfection of Surfaces. *J. Mater. Chem.* **2012**, *22*, 15388–15396.
- (25) Zhao, N.; Gao, X.; Chen, Z.; Feng, Y.; Liu, G.; Zhou, F.; Liu, W. Super-Lubricating Hybrid Elastomer with Rapid Photothermal Sterilization and Strong Anti-Cell Adhesion. *Chem. Eng. J.* **2022**, *434*, 134763.
- (26) Li, X.; Li, S.; Bai, Q.; Sui, N.; Zhu, Z. Gold Nanoclusters Decorated Amine-Functionalized Graphene Oxide Nanosheets for Capture, Oxidative Stress, and Photothermal Destruction of Bacteria. *Colloids Surf. B Biointerfaces* **2020**, *196*, 111313.
- (27) Khantamat, O.; Li, C.-H.; Yu, F.; Jamison, A. C.; Shih, W.-C.; Cai, C.; Lee, T. R. Gold Nanoshell-Decorated Silicone Surfaces for the near-Infrared (NIR) Photothermal Destruction of the Pathogenic Bacterium *E. Faecalis*. *ACS Appl. Mater. Interfaces* **2015**, *7*, 3981–3993.
- (28) Chandna, S.; Thakur, N. S.; Kaur, R.; Bhaumik, J. Lignin-Bimetallic Nanoconjugate Doped pH-Responsive Hydrogels for Laser-Assisted Antimicrobial Photodynamic Therapy. *Biomacromolecules* **2020**, *21*, 3216–3230.
- (29) Mao, C.; Xiang, Y.; Liu, X.; Cui, Z.; Yang, X.; Yeung, K. W. K.; Pan, H.; Wang, X.; Chu, P. K.; Wu, S. Photo-Inspired Antibacterial Activity and Wound Healing Acceleration by Hydrogel Embedded with Ag/Ag@AgCl/ZnO Nanostructures. *ACS Nano* **2017**, *11*, 9010–9021.
- (30) Borzenkov, M.; Moros, M.; Tortiglione, C.; Bertoldi, S.; Contessi, N.; Faré, S.; Taglietti, A.; D'Agostino, A.; Pallavicini, P.; Collini, M.; Chirico, G. Fabrication of Photothermally Active Poly (Vinyl Alcohol) Films with Gold Nanostars for Antibacterial Applications. *Beilstein J. Nanotechnol.* **2018**, *9*, 2040–2048.
- (31) Li, J.; Wang, Y.; Yang, J.; Liu, W. Bacteria Activated-Macrophage Membrane-Coated Tough Nanocomposite Hydrogel with Targeted Photothermal Antibacterial Ability for Infected Wound Healing. *Chem. Eng. J.* **2021**, *420*, 127638.
- (32) Choi, W.; Park, J. Y.; Kim, Y. Photothermal Sterilization Cellulose Patch with Hollow Gold Nanoparticles. *J. Ind. Eng. Chem.* **2021**, *95*, 120–125.
- (33) Dai, T.; Huang, Y.-Y.; Hamblin, M. R. Photodynamic Therapy for Localized Infections—State of the Art. *Photodiagnosis Photodyn. Ther.* **2009**, *6*, 170–188.
- (34) Songca, S. P.; Adjei, Y. Applications of Antimicrobial Photodynamic Therapy against Bacterial Biofilms. *Int. J. Mol. Sci.* **2022**, *23*, 3209.
- (35) Hamblin, M. R.; Hasan, T. Photodynamic Therapy: A New Antimicrobial Approach to Infectious Disease? *Photochem. Photobiol. Sci.* **2004**, *3*, 436–450.
- (36) He, T.; Meng, C.; Adamu, H. Y.; Li, C.; Huang, Y.; Liu, Y.; Li, L.; Chen, S.; Zhen, D. Near-Infrared-Driven  $\beta$ -NaYF<sub>4</sub>:Yb,Tm,Gd/Ni-MOF Nanocomposites for Efficient Sterilization and Degradation of Organic Contaminants. *ACS Appl. Nano Mater.* **2023**, *6*, 21721–21732.
- (37) Gnanasekar, S.; Kasi, G.; He, X.; Zhang, K.; Xu, L.; Kang, E.-T. Recent Advances in Engineered Polymeric Materials for Efficient Photodynamic Inactivation of Bacterial Pathogens. *Bioact. Mater.* **2023**, *21*, 157–174.
- (38) Castano, A. P.; Demidova, T. N.; Hamblin, M. R. Mechanisms in Photodynamic Therapy: Part One—Photosensitizers, Photochemistry and Cellular Localization. *Photodiagnosis Photodyn. Ther.* **2004**, *1*, 279–293.
- (39) Wainwright, M.; Maisch, T.; Nonell, S.; Plaetzer, K.; Almeida, A.; Tegos, G. P.; Hamblin, M. R. Photoantimicrobials—Are We Afraid of the Light? *Lancet Infect. Dis.* **2017**, *17*, e49–e55.
- (40) Gois, M. M.; Kurachi, C.; Santana, E. J. B.; Mima, E. G. O.; Spolidório, D. M. P.; Pelino, J. E. P.; Salvador Bagnato, V. Susceptibility of *Staphylococcus Aureus* to Porphyrin-Mediated Photodynamic Antimicrobial Chemotherapy: An in Vitro Study. *Lasers Med. Sci.* **2010**, *25*, 391–395.
- (41) Hu, X.; Huang, Y.-Y.; Wang, Y.; Wang, X.; Hamblin, M. R. Antimicrobial Photodynamic Therapy to Control Clinically Relevant Biofilm Infections. *Front. Microbiol.* **2018**, *9*, 1299.
- (42) Agostinis, P.; Berg, K.; Cengel, K. A.; Foster, T. H.; Girotti, A. W.; Gollnick, S. O.; Hahn, S. M.; Hamblin, M. R.; Juzeniene, A.; Kessel, D.; Korbelik, M.; Moan, J.; Mroz, P.; Nowis, D.; Piette, J.; Wilson, B. C.; Golab, J. Photodynamic Therapy of Cancer: An Update. *CA. Cancer J. Clin.* **2011**, *61*, 250–281.
- (43) Lee, Y.-E. K.; Kopelman, R. Polymeric Nanoparticles for Photodynamic Therapy. *Biomed. Nanotechnol. Methods Protoc.* **2011**, *726*, 151–178.
- (44) Zhang, Y.; Huang, Y.; Chen, H.; Luo, X.; Zhang, J.; Wang, H.; Zou, Q.; Wang, S. Design of a Nanocomposite with Gold Nanoparticles as the Core and Casein-Templated Gold Nanoclusters as the Shell with Ultra-Low Protein Corona for Enhanced Photodynamic Therapy. *Mater. Adv.* **2022**, *3*, 8438–8448.
- (45) Kodedová, M.; Liška, V.; Mosinger, J.; Sychrová, H. Light-Induced Antifungal Activity of Nanoparticles with an Encapsulated Porphyrin Photosensitizer. *Microbiol. Res.* **2023**, *269*, 127303.
- (46) Chatterjee, D. K.; Fong, L. S.; Zhang, Y. Nanoparticles in Photodynamic Therapy: An Emerging Paradigm. *Adv. Drug Delivery Rev.* **2008**, *60*, 1627–1637.
- (47) Shang, L.; Zhou, X.; Zhang, J.; Shi, Y.; Zhong, L. Metal Nanoparticles for Photodynamic Therapy: A Potential Treatment for Breast Cancer. *Molecules* **2021**, *26*, 6532.
- (48) Bacali, C.; Carpa, R.; Buduru, S.; Moldovan, M. L.; Baldea, I.; Constantin, A.; Moldovan, M.; Prodan, D.; Dascalu, L. M.; Lucaciu, O.; Catoi, F.; Constantiniu, M.; Badea, M. Association of Graphene Silver Polymethyl Methacrylate (PMMA) with Photodynamic Therapy for Inactivation of Halitosis Responsible Bacteria in Denture Wearers. *Nanomaterials* **2021**, *11*, 1643.
- (49) Bacali, C.; Baldea, I.; Moldovan, M.; Carpa, R.; Olteanu, D. E.; Filip, G. A.; Nastase, V.; Lascu, L.; Badea, M.; Constantiniu, M.; Badea, F. Flexural Strength, Biocompatibility, and Antimicrobial Activity of a Polymethyl Methacrylate Denture Resin Enhanced with Graphene and Silver Nanoparticles. *Clin. Oral Investig.* **2020**, *24*, 2713–2725.
- (50) Ozkan, E.; Allan, E.; Parkin, I. P. White-Light-Activated Antibacterial Surfaces Generated by Synergy between Zinc Oxide Nanoparticles and Crystal Violet. *ACS Omega* **2018**, *3*, 3190–3199.
- (51) Li, Q.; Liu, J.; Xu, Y.; Liu, H.; Zhang, J.; Wang, Y.; Sun, Y.; Zhao, M.; Liao, L.; Wang, X. Fast Cross-Linked Hydrogel as a Green Light-Activated Photocatalyst for Localized Biofilm Disruption and Brush-Free Tooth Whitening. *ACS Appl. Mater. Interfaces* **2022**, *14*, 28427–28438.
- (52) Sadowski, R.; Strus, M.; Buchalska, M.; Heczko, P. B.; Macyk, W. Visible Light Induced Photocatalytic Inactivation of Bacteria by



Modified Titanium Dioxide Films on Organic Polymers. *Photochem. Photobiol. Sci.* **2015**, *14*, 514–519.

(53) Sehmi, S. K.; Noimark, S.; Bear, J. C.; Peveler, W. J.; Bovis, M.; Allan, E.; MacRobert, A. J.; Parkin, I. P. Lethal Photosensitisation of Staphylococcus Aureus and Escherichia Coli Using Crystal Violet and Zinc Oxide-Encapsulated Polyurethane. *J. Mater. Chem. B* **2015**, *3*, 6490–6500.

(54) Noimark, S.; Weiner, J.; Noor, N.; Allan, E.; Williams, C. K.; Shaffer, M. S.; Parkin, I. P. Dual-Mechanism Antimicrobial Polymer-ZnO Nanoparticle and Crystal Violet-encapsulated Silicone. *Adv. Funct. Mater.* **2015**, *25*, 1367–1373.

(55) Ozkan, E.; Ozkan, F. T.; Allan, E.; Parkin, I. P. The Use of Zinc Oxide Nanoparticles to Enhance the Antibacterial Properties of Light-Activated Polydimethylsiloxane Containing Crystal Violet. *RSC Adv.* **2015**, *5*, 8806–8813.

(56) Chauhan, A.; Rastogi, M.; Scheier, P.; Bowen, C.; Kumar, R. V.; Vaish, R. Janus Nanostructures for Heterogeneous Photocatalysis. *Appl. Phys. Rev.* **2018**, *5*, 041111.

(57) Panwar, K.; Jassal, M.; Agrawal, A. K. TiO<sub>2</sub>-SiO<sub>2</sub> Janus Particles with Highly Enhanced Photocatalytic Activity. *RSC Adv.* **2016**, *6*, 92754–92764.

(58) Chen, Y.; Gao, Y.; Chen, Y.; Liu, L.; Mo, A.; Peng, Q. Nanomaterials-Based Photothermal Therapy and Its Potentials in Antibacterial Treatment. *J. Controlled Release* **2020**, *328*, 251–262.

(59) Borzenkov, M.; Pallavicini, P.; Taglietti, A.; D'Alfonso, L.; Collini, M.; Chirico, G. Photothermally Active Nanoparticles as a Promising Tool for Eliminating Bacteria and Biofilms. *Beilstein J. Nanotechnol.* **2020**, *11*, 1134–1146.

(60) Borzenkov, M.; Pallavicini, P.; Chirico, G. Photothermally Active Inorganic Nanoparticles: From Colloidal Solutions to Photothermally Active Printed Surfaces and Polymeric Nanocomposite Materials. *Eur. J. Inorg. Chem.* **2019**, *2019*, 4397–4404.

(61) Estelrich, J.; Busquets, M. A. Iron Oxide Nanoparticles in Photothermal Therapy. *Molecules* **2018**, *23*, 1567.

(62) de Aberasturi, D. J.; Serrano-Montes, A. B.; Liz-Marzán, L. M. Modern Applications of Plasmonic Nanoparticles: From Energy to Health. *Adv. Opt. Mater.* **2015**, *3*, 602–617.

(63) Ngo, N. M.; Tran, H.-V.; Lee, T. R. Plasmonic Nanostars: Systematic Review of Their Synthesis and Applications. *ACS Appl. Nano Mater.* **2022**, *5*, 14051.

(64) Zhao, B.; Chen, S.; Hong, Y.; Jia, L.; Zhou, Y.; He, X.; Wang, Y.; Tian, Z.; Yang, Z.; Gao, D. Research Progress of Conjugated Nanomedicine for Cancer Treatment. *Pharmaceutics* **2022**, *14*, 1522.

(65) Ren, Y.; Liu, H.; Liu, X.; Zheng, Y.; Li, Z.; Li, C.; Yeung, K. W. K.; Zhu, S.; Liang, Y.; Cui, Z.; Wu, S. Photoresponsive Materials for Antibacterial Applications. *Cell Rep. Phys. Sci.* **2020**, *1*, 100245.

(66) Yu, S.; Li, G.; Zhao, P.; Cheng, Q.; He, Q.; Ma, D.; Xue, W. NIR-laser-controlled Hydrogen-releasing PdH Nanohydride for Synergistic Hydrogen-photothermal Antibacterial and Wound-healing Therapies. *Adv. Funct. Mater.* **2019**, *29*, 1905697.

(67) Yu, Y.; Li, P.; Zhu, C.; Ning, N.; Zhang, S.; Vancso, G. J. Multifunctional and Recyclable Photothermally Responsive Cryogels as Efficient Platforms for Wound Healing. *Adv. Funct. Mater.* **2019**, *29*, 1904402.

(68) Ramasamy, M.; Lee, J. Recent Nanotechnology Approaches for Prevention and Treatment of Biofilm-Associated Infections on Medical Devices. *BioMed. Res. Int.* **2016**, *2016*, 1.

(69) Li, C.; Ye, R.; Bouckaert, J.; Zurutuza, A.; Drider, D.; Dumych, T.; Paryzhak, S.; Vovk, V.; Bilyy, R. O.; Melinte, S.; Li, M.; Boukherroub, R.; Szunerits, S. Flexible Nanohole Patches for Antibiotic-Free Treatments of Skin Infections. *ACS Appl. Mater. Interfaces* **2017**, *9*, 36665–36674.

(70) Han, S.; Han, K.; Hong, J.; Yoon, D.-Y.; Park, C.; Kim, Y. Photothermal Cellulose-Patch with Gold-Spiked Silica Microrods Based on Escherichia Coli. *ACS Omega* **2018**, *3*, 5244–5251.

(71) Zhang, W.; Kuang, Z.; Song, P.; Li, W.; Gui, L.; Tang, C.; Tao, Y.; Ge, F.; Zhu, L. Synthesis of a Two-Dimensional Molybdenum Disulfide Nanosheet and Ultrasensitive Trapping of *Staphylococcus*

*aureus* for Enhanced Photothermal and Antibacterial Wound-Healing Therapy. *Nanomaterials* **2022**, *12*, 1865.

(72) Wu, Z.; Zhuang, H.; Ma, B.; Xiao, Y.; Koc, B.; Zhu, Y.; Wu, C. Manganese-Doped Calcium Silicate Nanowire Composite Hydrogels for Melanoma Treatment and Wound Healing. *Research* **2021**, *2021*, No. 9780943.

(73) Hu, B.; Berkey, C.; Feliciano, T.; Chen, X.; Li, Z.; Chen, C.; Amini, S.; Nai, M. H.; Lei, Q.; Ni, R.; Wang, J.; Leow, W. R.; Pan, S.; Li, Y.-Q.; Cai, P.; Miserez, A.; Li, S.; Lim, C. T.; Wu, Y.-L.; Odom, T. W.; Dauskardt, R. H.; Chen, X. Thermal-Disrupting Interface Mitigates Intercellular Cohesion Loss for Accurate Topical Antibacterial Therapy. *Adv. Mater.* **2020**, *32*, 1907030.

(74) Liu, Y.; Li, F.; Guo, Z.; Xiao, Y.; Zhang, Y.; Sun, X.; Zhe, T.; Cao, Y.; Wang, L.; Lu, Q.; Wang, J. Silver Nanoparticle-Embedded Hydrogel as a Photothermal Platform for Combating Bacterial Infections. *Chem. Eng. J.* **2020**, *382*, 122990.

(75) Chen, S.; Tang, F.; Tang, L.; Li, L. Synthesis of Cu-Nanoparticle Hydrogel with Self-Healing and Photothermal Properties. *ACS Appl. Mater. Interfaces* **2017**, *9*, 20895–20903.

(76) Tao, B.; Lin, C.; Deng, Y.; Yuan, Z.; Shen, X.; Chen, M.; He, Y.; Peng, Z.; Hu, Y.; Cai, K. Copper-Nanoparticle-Embedded Hydrogel for Killing Bacteria and Promoting Wound Healing with Photothermal Therapy. *J. Mater. Chem. B* **2019**, *7*, 2534–2548.

(77) Ren, Y.; Yan, B.; Wang, P.; Yu, Y.; Cui, L.; Zhou, M.; Wang, Q. Construction of a Rapid Photothermal Antibacterial Silk Fabric via QCS-Guided In Situ Deposition of CuSNPs. *ACS Sustain. Chem. Eng.* **2022**, *10*, 2192–2203.

(78) Ren, Y.; Yan, B.; Lin, C.; Wang, P.; Zhou, M.; Cui, L.; Yu, Y.; Wang, Q. Multifunctional Textile Constructed via Polyaniline-Mediated Copper Sulfide Nanoparticle Growth for Rapid Photothermal Antibacterial and Antioxidation Applications. *ACS Appl. Nano Mater.* **2023**, *6*, 1212.

(79) de Miguel, I.; Prieto, I.; Albornoz, A.; Sanz, V.; Weis, C.; Turon, P.; Quidant, R. Plasmon-Based Biofilm Inhibition on Surgical Implants. *Nano Lett.* **2019**, *19*, 2524–2529.

(80) Zhao, Y.-Q.; Xiu, Z.; Wu, R.; Zhang, L.; Ding, X.; Zhao, N.; Duan, S.; Xu, F.-J. A Near-Infrared-Responsive Quaternary Ammonium/Gold Nanorod Hybrid Coating with Enhanced Antibacterial Properties. *Adv. NanoBiomed Res.* **2022**, *2*, 2200111.

(81) Grisoli, P.; De Vita, L.; Milanese, C.; Taglietti, A.; Diaz Fernandez, Y.; Bouzin, M.; D'Alfonso, L.; Sironi, L.; Rossi, S.; Vigani, B.; Sperandio, P.; Polissi, A.; Pallavicini, P. PVA Films with Mixed Silver Nanoparticles and Gold Nanostars for Intrinsic and Photothermal Antibacterial Action. *Nanomaterials* **2021**, *11*, 1387.

(82) Merkl, P.; Zhou, S.; Zaganianis, A.; Shahata, M.; Eleftheraki, A.; Thersleff, T.; Sotiriou, G. A. Plasmonic Coupling in Silver Nanoparticle Aggregates and Their Polymer Composite Films for Near-Infrared Photothermal Biofilm Eradication. *ACS Appl. Nano Mater.* **2021**, *4*, 5330–5339.

(83) Zhang, Y.; Yang, D.; Qiu, X.; Li, Z. UV-Assisted Room-Temperature Fabrication of Lignin-Based Nanosilver Complexes for Photothermal-Mediated Sterilization. *ACS Appl. Bio Mater.* **2022**, *5*, 5943–5952.

(84) Chen, Q.; Li, S.; Zhao, W.; Zhao, C. A Rapid-Triggered Approach towards Antibacterial Hydrogel Wound Dressing with Synergic Photothermal and Sterilization Profiles. *Biomater. Adv.* **2022**, *138*, 212873.

(85) Lin, X.; Fang, Y.; Hao, Z.; Wu, H.; Zhao, M.; Wang, S.; Liu, Y. Bacteria-Triggered Multifunctional Hydrogel for Localized Chemodynamic and Low-Temperature Photothermal Sterilization. *Small* **2021**, *17*, 2103303.

(86) Zhou, R.; Zhou, Q.; Ling, G.; Zhang, P. A Cross-Linked Hydrogel of Bismuth Sulfide Nanoparticles with Excellent Photothermal Antibacterial and Mechanical Properties to Combat Bacterial Infection and Prompt Wound Healing. *Colloids Surf. Physicochem. Eng. Asp.* **2023**, *660*, 130832.

(87) Ma, B.; Dang, W.; Yang, Z.; Chang, J.; Wu, C. MOS<sub>2</sub> Nanoclusters-Based Biomaterials for Disease-Impaired Wound Therapy. *Appl. Mater. Today* **2020**, *20*, 100735.

- (88) Chen, J.; Ning, C.; Zhou, Z.; Yu, P.; Zhu, Y.; Tan, G.; Mao, C. Nanomaterials as Photothermal Therapeutic Agents. *Prog. Mater. Sci.* **2019**, *99*, 1–26.
- (89) Hong, G.; Diao, S.; Chang, J.; Antaris, A. L.; Chen, C.; Zhang, B.; Zhao, S.; Atochin, D. N.; Huang, P. L.; Andreasson, K. I.; Kuo, C. J.; Dai, H. Through-Skull Fluorescence Imaging of the Brain in a New near-Infrared Window. *Nat. Photonics* **2014**, *8*, 723–730.
- (90) Won, N.; Jeong, S.; Kim, K.; Kwag, J.; Park, J.; Kim, S. G.; Kim, S. Imaging Depths of Near-Infrared Quantum Dots in First and Second Optical Windows. *Mol. Imaging* **2012**, *11*, 7290–2011.
- (91) Melamed, J. R.; Edelstein, R. S.; Day, E. S. Elucidating the Fundamental Mechanisms of Cell Death Triggered by Photothermal Therapy. *ACS Nano* **2015**, *9*, 6–11.
- (92) Hu, X.; Zhang, H.; Wang, Y.; Shiu, B.-C.; Lin, J.-H.; Zhang, S.; Lou, C.-W.; Li, T.-T. Synergistic Antibacterial Strategy Based on Photodynamic Therapy: Progress and Perspectives. *Chem. Eng. J.* **2022**, *450*, 138129.
- (93) Wang, R.; Kim, D.; Yang, M.; Li, X.; Yoon, J. Phthalocyanine-Assembled “One-For-Two” Nanoparticles for Combined Photodynamic-Photothermal Therapy of Multidrug-Resistant Bacteria. *ACS Appl. Mater. Interfaces* **2022**, *14*, 7609–7616.
- (94) Mutalik, C.; Okoro, G.; Krisnawati, D. I.; Jazidie, A.; Rahmawati, E. Q.; Rahayu, D.; Hsu, W.-T.; Kuo, T.-R. Copper Sulfide with Morphology-Dependent Photodynamic and Photothermal Antibacterial Activities. *J. Colloid Interface Sci.* **2022**, *607*, 1825–1835.
- (95) Zhang, W.; Shen, X.; Li, W.; Wang, J.; Kuang, Z.; Gui, L.; Tao, Y.; Song, P.; Ge, F.; Zhu, L. Antibacterial MoS<sub>2</sub>-Ce6-Ionic Liquid Nanoplatfrom against Photothermal/Photodynamic Combined Therapy and Wound Healing Acceleration. *ACS Appl. Nano Mater.* **2023**, *6*, 20556–20568.
- (96) Qian, G.; Wen, T.; Shuai, Y.; Wu, X.; Zeng, Z.; Peng, S.; Shuai, C. Photothermal and Photodynamic Effects of G-C<sub>3</sub>N<sub>4</sub> Nanosheet/Bi<sub>2</sub>S<sub>3</sub> Nanorod Composites with Antibacterial Activity for Tracheal Injury Repair. *ACS Appl. Nano Mater.* **2022**, *5*, 16528–16543.
- (97) Hang, L.; Zhang, T.; Wen, H.; Liang, L.; Li, W.; Ma, X.; Jiang, G. Controllable Photodynamic Performance via an Acidic Micro-environment Based on Two-Dimensional Metal-Organic Frameworks for Photodynamic Therapy. *Nano Res.* **2021**, *14*, 660–666.
- (98) Jia, Q.; Song, Q.; Li, P.; Huang, W. Rejuvenated Photodynamic Therapy for Bacterial Infections. *Adv. Healthc. Mater.* **2019**, *8*, 1900608.
- (99) Liu, Y.; Liu, F.; Qiu, Y.; Li, Z.; Wei, Q.; Zhang, N.; Ma, C.; Xu, W.; Wang, Y. Potent Antibacterial Fibers with the Functional “Triad” of Photothermal, Silver, and Dex for Bone Infections. *Mater. Des.* **2022**, *223*, 111153.
- (100) Zhang, X.; Zhang, C.; Yang, Y.; Zhang, H.; Huang, X.; Hang, R.; Yao, X. Light-Assisted Rapid Sterilization by a Hydrogel Incorporated with Ag<sub>3</sub>PO<sub>4</sub>/MoS<sub>2</sub> Composites for Efficient Wound Disinfection. *Chem. Eng. J.* **2019**, *374*, 596–604.
- (101) Li, M.; Liu, X.; Tan, L.; Cui, Z.; Yang, X.; Li, Z.; Zheng, Y.; Yeung, K. W. K.; Chu, P. K.; Wu, S. Noninvasive Rapid Bacteria-Killing and Acceleration of Wound Healing through Photothermal/Photodynamic/Copper Ion Synergistic Action of a Hybrid Hydrogel. *Biomater. Sci.* **2018**, *6*, 2110–2121.
- (102) Zhang, J.; Gao, X.; Ma, D.; He, S.; Du, B.; Yang, W.; Xie, K.; Xie, L.; Deng, Y. Copper Ferrite Heterojunction Coatings Empower Polyetheretherketone Implant with Multi-Modal Bactericidal Functions and Boosted Osteogenicity through Synergistic Photo/Fenton-Therapy. *Chem. Eng. Trans* **2021**, *422*, 130094.
- (103) Xie, Y.; Gan, C.; Li, Z.; Liu, W.; Yang, D.; Qiu, X. Fabrication of a Lignin-Copper Sulfide-Incorporated PVA Hydrogel with Near-Infrared-Activated Photothermal/Photodynamic/Peroxidase-like Performance for Combating Bacteria and Biofilms. *ACS Biomater. Sci. Eng.* **2022**, *8*, S60–S69.
- (104) Feng, Z.; Liu, X.; Tan, L.; Cui, Z.; Yang, X.; Li, Z.; Zheng, Y.; Yeung, K. W. K.; Wu, S. Electrophoretic Deposited Stable Chitosan@MoS<sub>2</sub> Coating with Rapid in Situ Bacteria-killing Ability under Dual-light Irradiation. *Small* **2018**, *14*, 1704347.
- (105) Yuan, Z.; Tao, B.; He, Y.; Liu, J.; Lin, C.; Shen, X.; Ding, Y.; Yu, Y.; Mu, C.; Liu, P.; Cai, K. Biocompatible MoS<sub>2</sub>/PDA-RGD Coating on Titanium Implant with Antibacterial Property via Intrinsic ROS-Independent Oxidative Stress and NIR Irradiation. *Biomaterials* **2019**, *217*, 119290.
- (106) Zhang, X.; Zhang, G.; Zhang, H.; Liu, X.; Shi, J.; Shi, H.; Yao, X.; Chu, P. K.; Zhang, X. A Bifunctional Hydrogel Incorporated with CuS@MoS<sub>2</sub> Microspheres for Disinfection and Improved Wound Healing. *Chem. Eng. J.* **2020**, *382*, 122849.
- (107) Sun, J.; Song, L.; Fan, Y.; Tian, L.; Luan, S.; Niu, S.; Ren, L.; Ming, W.; Zhao, J. Synergistic Photodynamic and Photothermal Antibacterial Nanocomposite Membrane Triggered by Single NIR Light Source. *ACS Appl. Mater. Interfaces* **2019**, *11*, 26581–26589.
- (108) Cui, Q.; Yuan, H.; Bao, X.; Ma, G.; Wu, M.; Xing, C. Synergistic Photodynamic and Photothermal Antibacterial Therapy Based on a Conjugated Polymer Nanoparticle-Doped Hydrogel. *ACS Appl. Bio Mater.* **2020**, *3*, 4436–4443.
- (109) Gao, D.; Ji, X.; Wang, J.; Wang, Y.; Li, D.; Liu, Y.; Chang, K.; Qu, J.; Zheng, J.; Yuan, Z. Engineering a Protein-Based Nanoplatfrom as an Antibacterial Agent for Light Activated Dual-Modal Photothermal and Photodynamic Therapy of Infection in Both the NIR I and II Windows. *J. Mater. Chem. B* **2018**, *6*, 732–739.
- (110) Zhang, Y.; Ma, J.; Wang, D.; Xu, C.; Sheng, S.; Cheng, J.; Bao, C.; Li, Y.; Tian, H. Fe-TCPP@CS Nanoparticles as Photodynamic and Photothermal Agents for Efficient Antimicrobial Therapy. *Biomater. Sci.* **2020**, *8*, 6526–6532.
- (111) Xie, G.; Wang, X.; Mo, M.; Zhang, L.; Zhu, J. Photothermal Hydrogels for Promoting Infected Wound Healing. *Macromol. Biosci.* **2023**, *23*, 2200378.
- (112) Hou, Y.; Yang, X.; Liu, R.; Zhao, D.; Guo, C.; Zhu, A.; Wen, M.; Liu, Z.; Qu, G.; Meng, H. Pathological Mechanism of Photodynamic Therapy and Photothermal Therapy Based on Nanoparticles. *Int. J. Nanomedicine* **2020**, *15*, 6827–6838.
- (113) Fasciani, C.; Silvero, M. J.; Anghel, M. A.; Argüello, G. A.; Becerra, M. C.; Scaiano, J. C. Aspartame-Stabilized Gold-Silver Bimetallic Biocompatible Nanostructures with Plasmonic Photothermal Properties, Antibacterial Activity, and Long-Term Stability. *J. Am. Chem. Soc.* **2014**, *136*, 17394–17397.
- (114) Wei, G.; Yang, G.; Wang, Y.; Jiang, H.; Fu, Y.; Yue, G.; Ju, R. Phototherapy-Based Combination Strategies for Bacterial Infection Treatment. *Theranostics* **2020**, *10*, 12241.